



OKLAHOMA TRANSPORTATION CENTER

ECONOMIC ENHANCEMENT THROUGH INFRASTRUCTURE STEWARDSHIP

USE OF MSE TECHNOLOGY TO STABILIZE HIGHWAY EMBANKMENTS AND SLOPES IN OKLAHOMA

KIANOOSH HATAMI, PH.D.
GERALD A. MILLER, PH.D.
LINA M. GARCIA

OTCREOS7.1-19-F

Oklahoma Transportation Center
2601 Liberty Parkway, Suite 110
Midwest City, Oklahoma 73110

Phone: 405.732.6580
Fax: 405.732.6586
www.oktc.org

DISCLAIMER

The contents of this report reflect the views of the authors, who are responsible for the facts and accuracy of the information presented herein. This document is disseminated under the sponsorship of the Department of Transportation University Transportation Centers Program, in the interest of information exchange. The U.S. Government assumes no liability for the contents or use thereof.

1. REPORT NO. OTCREOS7.1-19-F	2. GOVERNMENT ACCESSION NO.	3. RECIPIENTS CATALOG NO.	
4. TITLE AND SUBTITLE Use of MSE Technology to Stabilize Highway Embankments and Slopes in Oklahoma		5. REPORT DATE September 30, 2009	
7. AUTHOR(S) Kianoosh Hatami, Gerald A. Miller and Lina M. Garcia		6. PERFORMING ORGANIZATION CODE	
9. PERFORMING ORGANIZATION NAME AND ADDRESS The University of Oklahoma School of Civil Engineering and Environmental Engineering Norman, OK 73110		8. PERFORMING ORGANIZATION REPORT	
12. SPONSORING AGENCY NAME AND ADDRESS Oklahoma Transportation Center (Fiscal) 201 ARRC Stillwater, OK 74078 (Technical) 2601 Liberty Parkway, Suite 110 Midwest City, OK 73110		10. WORK UNIT NO.	
15. SUPPLEMENTARY NOTES University Transportation Center		11. CONTRACT OR GRANT NO. DTRT06-G-0016	
16. ABSTRACT Departments of transportation across the U.S., including ODOT, are invariably faced with a persistent problem of landslides and slope failures along highways. Repairs and maintenance work associated with these failures cost these agencies millions of dollars annually. An ideal solution for the construction or repair of slopes and embankments is to use large quantities of coarse-grained, free-draining soils to stabilize these structures. However, such soils are not readily available in Oklahoma and many other parts of the U.S. Consequently, the production and transportation costs for these materials can be prohibitive amounting to millions of dollars annually. A possible solution to this problem would be to use locally available soils that are of marginal quality (e.g. soils with more than 15% fines content) but are significantly less expensive. However, the pullout capacity of reinforcement in reinforced soil slopes constructed with marginal soils can decrease as a result of increase in the soil moisture content. The loss of matric suction and excess pore water pressure as a result of compaction or prolonged precipitation during construction or service life of the structure can jeopardize the stability of structure or lead to excessive deformation. Current design guidelines for reinforced soil slopes in North America do not account for the reduction in the interface strength due to increased moisture content. This study is aimed at developing a moisture reduction factor (MRF) to account for the influence of moisture content on the soil-geosynthetic reinforcement interface strength in reinforced soil structures constructed with marginal soils. In this one-year study, MRF values were determined for an Oklahoma marginal soil and a woven geotextile reinforcement material through large-scale and small-scale pullout tests. The tests were carried out at three different moisture content values: optimum moisture content (OMC), OMC+2% and OMC-2%. It was found that the strength of soil-geotextile reinforcement interface constructed at OMC-2% could decrease by as much as 20%-40% when the soil moisture content is increased to OMC+2%. The outcome of this long-term study will assist ODOT and other departments of transportation in the U.S. to include the influence of soil moisture content in their stability analysis and design of reinforced soil structures to repair, stabilize and reconstruct slopes composed of marginal soils along the transportation corridors in the U.S.		13. TYPE OF REPORT AND PERIOD COVERED Final August 2008 – September 2009	
17. KEY WORDS Soil-Reinforcement Interface, Unsaturated Soil, Soil Suction, Pullout, Reinforced Soil Slopes, Slope Stability		18. DISTRIBUTION STATEMENT No restrictions. This publication is available at www.oktc.org and from NTIS.	
19. SECURITY CLASSIF. (OF THIS REPORT) Unclassified	20. SECURITY CLASSIF. (OF THIS PAGE) Unclassified	21. NO. OF PAGES 61 + covers	22. PRICE

ACKNOWLEDGEMENTS

The funding for this study was provided through the Oklahoma Transportation Center Award No. OTCREOS7.1-19 and ODOT Award No. SPR 2214. The authors are grateful for their useful discussions with ODOT engineers Mr. Jeff Dean, Drs. Butch Reidenbach and Jim Nevels, and Mr. Chris Clarke over the course of this study. The geotextile was donated by TenCate Geosynthetics. Undergraduate research assistants, Lee Blackburn, Matt Long, Derek Reid, Kyle Olson, Max Newton and Jeremy Christiansen helped with the setup and execution of the tests. The assistance of Mr. Michael Schmitz at the OU Fears Structural Laboratory is gratefully acknowledged.

SI (METRIC) CONVERSION FACTORS

Approximate Conversions to SI Units				
Symbol	When you know	Multiply by	To Find	Symbol
LENGTH				
in	inches	25.40	millimeters	mm
ft	feet	0.3048	meters	m
yd	yards	0.9144	meters	m
mi	miles	1.609	kilometers	km
AREA				
in ²	square inches	645.2	square millimeters	mm ²
ft ²	square feet	0.0929	square meters	m ²
yd ²	square yards	0.8361	square meters	m ²
ac	acres	0.4047	hectares	ha
mi ²	square miles	2.590	square kilometers	km ²
VOLUME				
fl oz	fluid ounces	29.57	milliliters	mL
gal	gallons	3.785	liters	L
ft ³	cubic feet	0.0283	cubic meters	m ³
yd ³	cubic yards	0.7645	cubic meters	m ³
MASS				
oz	ounces	28.35	grams	g
lb	pounds	0.4536	kilograms	kg
T	short tons (2000 lb)	0.907	megagrams	Mg
TEMPERATURE (exact)				
°F	degrees Fahrenheit	(°F-32)/1.8	degrees Celsius	°C
FORCE and PRESSURE or STRESS				
lbf	poundforce	4.448	Newtons	N
lbf/in ²	poundforce per square inch	6.895	kilopascals	kPa

Approximate Conversions from SI Units				
Symbol	When you know	Multiply by	To Find	Symbol
LENGTH				
mm	millimeters	0.0394	inches	in
m	meters	3.281	feet	ft
m	meters	1.094	yards	yd
km	kilometers	0.6214	miles	mi
AREA				
mm ²	square millimeters	0.00155	square inches	in ²
m ²	square meters	10.764	square feet	ft ²
m ²	square meters	1.196	square yards	yd ²
ha	hectares	2.471	acres	ac
km ²	square kilometers	0.3861	square miles	mi ²
VOLUME				
mL	milliliters	0.0338	fluid ounces	fl oz
L	liters	0.2642	gallons	gal
m ³	cubic meters	35.315	cubic feet	ft ³
m ³	cubic meters	1.308	cubic yards	yd ³
MASS				
g	grams	0.0353	ounces	oz
kg	kilograms	2.205	pounds	lb
Mg	megagrams	1.1023	short tons (2000 lb)	T
TEMPERATURE (exact)				
°C	degrees Celsius	9/5+32	degrees Fahrenheit	°F
FORCE and PRESSURE or STRESS				
N	Newtons	0.2248	poundforce	lbf
kPa	kilopascals	0.1450	poundforce per square inch	lbf/in ²

Use of MSE Technology to Stabilize Highway Embankments and Slopes in Oklahoma

**FINAL REPORT
OTCREOS7.1-19-F**

Submitted to:

Oklahoma Transportation Center
2601 Liberty Parkway, Suite 110
Midwest City, Oklahoma 73110

Submitted by:

Kianoosh Hatami, Gerald A. Miller & Lina Garcia
School of Civil Engineering and Environmental Science
The University of Oklahoma
202 W. Boyd St., Room 334
Norman, OK 73019

TABLE OF CONTENTS

1. INTRODUCTION	12
2. THEORY.....	14
2.1. Reinforcement Pullout Capacity in MSE Structures	14
2.2. Extended Mohr-Coulomb Failure Envelope.....	15
3. MATERIAL PROPERTIES	16
3.1. Soil Properties	16
3.2. Geosynthetic Properties	20
4. LARGE-SCALE PULLOUT TESTS	21
4.1. Methodology	21
4.1.1. <i>Test Equipment</i>	21
4.1.2. <i>Instrumentation</i>	22
4.2. Large Scale Pullout Tests in Sand	24
4.2.1. <i>Interface friction angle</i>	26
4.3. Large-Scale Pullout Tests in Minco Silt.....	29
4.3.1. <i>Interface friction angle</i>	36
4.3.2. <i>Soil moisture content and suction</i>	38
4.3.3. <i>Parameters α and F^*</i>	44
5. SMALL-SCALE TESTS	46
5.1. Direct Shear Tests.....	47
5.1.1. <i>Results</i>	48
5.2. Pullout Tests.....	51
5.2.1. <i>Results</i>	52
6. MOISTURE REDUCTION FACTOR, $\mu(\omega)$.....	57
7. CONCLUSIONS	58
8. RECOMMENDATIONS AND TECHNOLOGY TRANSFER.....	58
9. REFERENCES	60

LIST OF FIGURES

Figure 1. Slope failures in Latimer County	12
Figure 2. Minco silt was found in west central Oklahoma.....	16
Figure 3. Uniformly graded fine sand drying process	16
Figure 4. Sand.....	17
Figure 5. Gradation curves (sieve analysis) of sand and Minco silt.....	17
Figure 6. Minco silt	18
Figure 7. Soil-Water Characteristic Curve (SWCC) for Minco silt (Tan 2005)	19
Figure 8. Standard Proctor test results on Minco silt.....	19
Figure 9. Geotextile (HP370).....	20
Figure 10. Mechanical response of geotextile (HP370) as per ASTM D4595 test protocol and as compared with the manufacturer's data.....	20
Figure 11. Pullout test box.....	22
Figure 12. (a) Tensiometer probes placed near the soil-geotextile interface, (b) tensiometer readout dials	23
Figure 13. (a) wire-line extensometers attached to the geotextile reinforcement (b) earth pressure cell placed at the top of the soil in the pullout test box	23
Figure 14. HP 370 Geotextile placed at the middle of the pullout box with wireline extensometers attached	24
Figure 15. A sideview of the soil and filler panels in the pullout box.....	24
Figure 16. Placement of earth pressure cell on the top of soil in the test box	24
Figure 17. A sideview of the pullout test box filled with soil	24
Figure 18. Comparison of load-displacement responses of geotextile reinforcement embedded in 6" and 8" of sand (Tests 2 and 3)	26
Figure 19. (a) Pullout test results on HP370 woven geotextile embedded in 200 mm (8") sand (b) overburden stress vs. pullout resistance	27
Figure 20. (a-c) Mechanical performance of the PP woven geotextile when pulled out under different overburden pressure magnitudes: (a) 68 kPa, (b) 50 kPa, (c) 10 kPa; (d) locations of telltales (extensometers) on the geotextile specimens.....	28
Figure 21. Pullout test results on HP370 woven geotextile embedded in 200 mm (8") sand including test 9 (peak pullout loads are marked with hollow circles).....	28

Figure 22. Mixing of Minco silt with water.....	30
Figure 23. Sieving processes.....	30
Figure 24. Soil samples in the oven (one sample per bucket) to determine their moisture content.....	30
Figure 25. Minco silt in 33 sealed buckets.....	30
Figure 26. Pullout box lined with plastic sheets.....	31
Figure 27. Pullout box set up.....	31
Figure 28.(a) Tensiometer probes placed near the soil-geotextile interface and wire-line extensometers attached to geotextile; (b) schematic diagram indicating the locations of tensiometers in the pullout test box; (c) tensiometer dial gauges.....	33
Figure 29. Schematic diagram of the pullout box.....	34
Figure 30. Moisture content within each layer inside the pullout box at OMC-2%, OMC and OMC+2% for each test.....	35
Figure 31. Regions within the test box where soil samples were taken to measure moisture content, (a) side view, (b) plan view.....	36
Figure 32. Pullout test data for Minco silt and interface strength results for Minco silt and comparison of failure envelopes for soil-geotextile Interface at different moisture contents (OMC-2%, OMC and OMC+2%).....	37
Figure 33. Suction data for pullout tests in Minco silt, the horizontal line in each graph Indicates the average suction value from Table 6.	40
Figure 34. Data for large-scale pullout tests in Minco Silt and comparison of failure envelopes of the soil-geotextile interface for determination of effective adhesion (c_a') and friction angle (δ^b) between soil and geotextile interface at different suctions.....	41
Figure 35. Extended Mohr-Coulomb failure envelopes for the soil-geotextile interface.	43
Figure 36. Large-scale pullout test in Minco silt was used to obtain pullout parameters for geotextile HP370 reinforcement and to obtain values for α and F^*	45
Figure 37. Direct shear test cell.....	47
Figure 38. Sand-geotextile interface shear test results: (a) mechanical response; (b) failure envelop.....	48
Figure 39. Direct shear test results in Minco silt.....	50
Figure 40. Direct shear in Minco silt.....	51
Figure 41. Small-scale pullout tests in Minco silt.....	52

Figure 42. Data for small-scale pullout tests in Minco silt and comparison of failure envelopes of the soil-geotextile interface for determination of effective adhesion (c_a') and friction angle (δ^b) between soil and geotextile interface at different suction values 53

Figure 43. Small-scale pullout test 54

Figure 44. Minco silt-geotextile interface strength results from pullout tests: (a) large-scale tests; (b) small-scale tests 56

Figure 45 Moisture reduction factor, $\mu(\omega)$, for Minco silt-woven geotextile from large-scale and small-scale pullout tests 57

LIST OF TABLES

Table 1. Sand properties	17
Table 2. Minco silt properties	18
Table 3. Large-scale pullout test cases and material properties	21
Table 4. Large-scale pullout tests in sand	25
Table 5. Pullout test results (200 mm soil embedment cases)	27
Table 6. Test information for large-scale pullout tests	32
Table 7. Interface strength properties from pullout tests in Minco silt.....	38
Table 8. Interface strength properties from pullout tests in Minco silt as a function of suction.....	42
Table 9. Large-scale pullout test in Minco to obtain values for α and F^*	44
Table 10. Small-scale test cases and material properties	47
Table 11. Sand strength properties from direct shear tests.....	49
Table 12. Minco silt strength properties from direct shear tests	51
Table 13. Interface strength properties from small-scale pullout tests.....	54

EXECUTIVE SUMMARY

Departments of transportation across the U.S., including ODOT, are invariably faced with a persistent problem of landslides and slope failures along highways. Repairs and maintenance work associated with these failures cost these agencies millions of dollars annually. An ideal solution for the construction or repair of slopes and embankments is to use large quantities of coarse-grained, free-draining soils to stabilize these structures. However, such coarse-grained soils are not readily available in Oklahoma and many other parts of the U.S. Consequently, the production and transportation costs for these materials can be prohibitive amounting to millions of dollars annually. A possible solution to this problem would be to use locally available soils that are of marginal quality (e.g. soils with more than 15% fines content) but are significantly less expensive.

One main concern in internal stability of reinforced soil slopes constructed with marginal soils is the pullout capacity of reinforcement when the soil moisture content increases significantly. This increase can occur as a result of soil compaction or prolonged precipitation during construction or service life of the structure. The reduction in normal effective stress and loss of interface shear strength has been reported to be responsible for excessive deformation or complete failure of reinforced soil structures. In spite of such possibilities and actual failure occurrences, current design guidelines and test protocols for reinforced soil slopes in North America do not include specific procedures to account for the reduction in interface strength due to increased moisture content.

This study is aimed at developing a moisture reduction factor (MRF) to account for the influence of moisture content on soil-geosynthetic reinforcement interface strength in reinforced soil structures constructed with marginal soils. In this one-year study, MRF values were determined for an Oklahoma marginal soil and a woven geotextile reinforcement material through large-scale and small-scale pullout tests. The tests were carried out at three different moisture content values: optimum moisture content (OMC), OMC+2% and OMC-2%. It was found that the strength of soil-geotextile reinforcement interface constructed at OMC-2% could decrease by as much as 20%-40% when the soil moisture content is increased to OMC+2%.

1. Introduction

Over many years there have been problems with slope failures and landslides along the highways in Oklahoma. Many of these failures occur in eastern Oklahoma due to steeper topography, soil types or a combination of both. A recent example of these failures is the massive slope failure on Highway 82 in Latimer County in southeastern Oklahoma. (**Figure 1**)



Figure 1. Slope failures in Latimer County

For construction or repair of these slopes and embankments the best solution would be to work with large quantities of coarse-grained, free-draining soils to stabilize the structures as recommended by design guidelines and specifications for Mechanically Stabilized Earth (MSE) structures in North America (Elias et al. 2001, AASHTO 2002). However, these specific soils are not commonly available in Oklahoma. Consequently, the cost of transportation and fill material can be very significant depending on the location of the high-quality soil.

One possible solution would be to use locally available soils as construction materials because they would require significantly less material transportation, fuel consumption and generated pollution compared to using high-quality offsite soils. It has been estimated that fuel costs constitute about 20% of the total costs for transportation of high-quality soil (Ou et al. 1982). On the other hand, commonly available soils in Oklahoma for the construction of reinforced slopes are of marginal quality (e.g., soils with more than 15% of fines content). Geosynthetic fabric can be used to stabilize marginal soils. Using the Mechanically Stabilized Earth technology (MSE) can help

reduce the cost of fill material by up to 60% (Keller 1995). However, in order to reinforce earthen structures involving marginal soils, it is important to obtain a satisfactory soil-reinforcement interface performance. Marginal soils and their interface with geosynthetic reinforcement can exhibit complex performance under construction or service loading conditions, including strain softening behavior and loss of strength and deformation as a result of wetting.

An important consideration in the design of reinforced soil structures constructed with marginal soils is the possibility of reduction in interface pullout resistance due to the increase in the soil moisture content (wetting). Increase in the soil moisture content could lead to loss of suction and development of excess pore water pressure. This can result in excessive deformations and even failure. As a result, the design procedures need to take into account the influence of soil moisture content on soil strength, the strength of soil-geosynthetic interface and the resulting factors of safety against failure. Such design provisions are currently not available for reinforced soil structures constructed with marginal soils. Typically, construction materials for reinforced soil structures are tested at moisture content values near optimum (i.e. Optimum Moisture Content - OMC). However, in actual construction, several factors could make the fill moisture content deviate from the design value. Examples include precipitation during construction, groundwater infiltration and development of excess pore water pressure due to compaction. These factors, in addition to seasonal variations of soil moisture content, can significantly reduce the strength of the soil-reinforcement interface and lead to excessive deformations or failure.

A primary objective of this study is to develop a moisture reduction factor (MRF) for the pullout resistance of soil-geotextile interfaces for the design of reinforced soil structures with marginal soils.

2. Theory

2.1. Reinforcement Pullout Capacity in MSE Structures

For internal stability, pullout resistance (per unit width), P_r , of the reinforcement is determined using **Equation 1** (Elias et al. 2001) and it is defined as the ultimate tensile load required to generate outward sliding of the reinforcement through the reinforced soil mass:

$$P_r = F^* \alpha \sigma'_v L_e C \quad (1)$$

where:

L_e = the embedment or adherence length in the resisting zone behind the failure surface

C = the reinforcement effective unit perimeter; e.g., $C = 2$ for strips, grids, and sheets

$L_e * C$ = the total surface area per unit width of the reinforcement in the resistive zone behind the failure surface

$F^* = \tan \delta_{\text{peak}}$ = the pullout resistance factor

δ_{peak} = equivalent peak friction angle of the soil-geosynthetic interface

α = a scale effect correction factor to account for a nonlinear stress reduction over the embedded length of highly extensible reinforcements.

σ'_v = the effective vertical stress at the soil-reinforcement interfaces.

A pullout test can be used to obtain pullout parameters for extensible reinforcements and to obtain values for α and F^* . The correction factor α depends on the extensibility and the length of the reinforcement, for extensible sheets (i.e., geotextile) the recommended value of α is 0.6. The parameter F^* (especially in reinforcement types such as geogrids and welded wire mesh) includes both passive and frictional resistance components (e.g., Palmeira 2004, Abu-Farsakh et al. 2005).

Pullout tests provide a short-term pullout capacity and do not account for soil or reinforcement creep deformations. Tests should be performed on samples with a minimum embedded length of 600 mm (24") as recommended in guidelines. The pullout resistance (P_r) is taken as the peak pullout resistance value from the pullout tests.

2.2. Extended Mohr-Coulomb Failure Envelope

The shear strength of an unsaturated soil depends on two stress variables: net normal stress ($\sigma_n - u_a$) and soil matric suction ($u_a - u_w$) (Fredlund et al. 1978). Net normal stress is the difference between the total stress and pore air pressure, and the matric suction is the difference between the pore air and the pore water pressures. This theory is also valid for dry and saturated soil conditions. The unsaturated shear strength of the soil-structure interface is determined using the following equation (Miller and Hamid 2005):

$$\tau_s = c'_a + (\sigma_n - u_a)\tan \delta' + (u_a - u_w)\tan \delta^b \quad (2)$$

c'_a = adhesion intercept

σ_n = normal stress on the interface,

u_a = pore air pressure.

δ' = the angle of friction between soil and reinforcement with respect to the σ_n abscissa.

u_w = pore water pressure.

δ^b = the angle of friction between soil and reinforcement with respect to the suction ($u_a - u_w$) abscissa.

In the case of unsaturated soil, the Mohr circles representing failure conditions correspond to a 3D failure envelop, where the shear stress (t) is the ordinate and the two stress variables are the abscissas ($\sigma_n - u_a$ and $u_a - u_w$). The locations of the Mohr circles in the third dimension are functions of matric suction ($u_a - u_w$). The planar surface formed by these two stress variables is called the extended Mohr-Coulomb failure envelop.

3. Material Properties

3.1. Soil Properties

Two different soils were used in the pullout tests carried out in this study: a uniformly graded fine sand available at the OU Fears Laboratory (in the control tests) and a fine-grained soil called Minco silt. The gradation and material properties of the sand are given in **Table 1** and **Figure 5**. The uniformity coefficient (C_u) of the sand is less than 3, which makes the sand classified as uniformly graded. Minco silt was found in west central Oklahoma about 20 miles west of El Reno (south of Geary) (**Figure 2**) just inside the Canadian County. Physical and mechanical soil property tests were carried out on Minco silt samples and compared to the results reported by Tan (2005) as shown in **Table 2**. Minco silt was found to be ideal for an unsaturated soil study due to its lower cohesion and matric suction compared to clayey soils. It allowed the use of tensiometers which are suitable for measuring suction values up to about 100 kPa. Minco Silt is classified as a CL-ML soil according to the Unified Soil Classification System (USCS).



Figure 2. Minco silt was found in west central Oklahoma



Figure 3. Uniformly graded fine sand drying process

The physical properties, textural composition and engineering properties of the soils used in the study are shown in **Tables 1 and 2** and **Figures 4 through 8**.

Table 1. Sand properties

<i>Sand (SP)</i>	
<i>Gravel, %</i>	0
<i>Sand, %</i>	98
<i>Fines, %</i>	2
<i>Maximum Dry Unit Weight, kN/m³ (pcf)</i>	17.9 (114)
<i>Optimum Moisture Content, %</i>	12.5
<i>C_c</i>	0.9
<i>C_u</i>	1.56



Figure 4. Sand

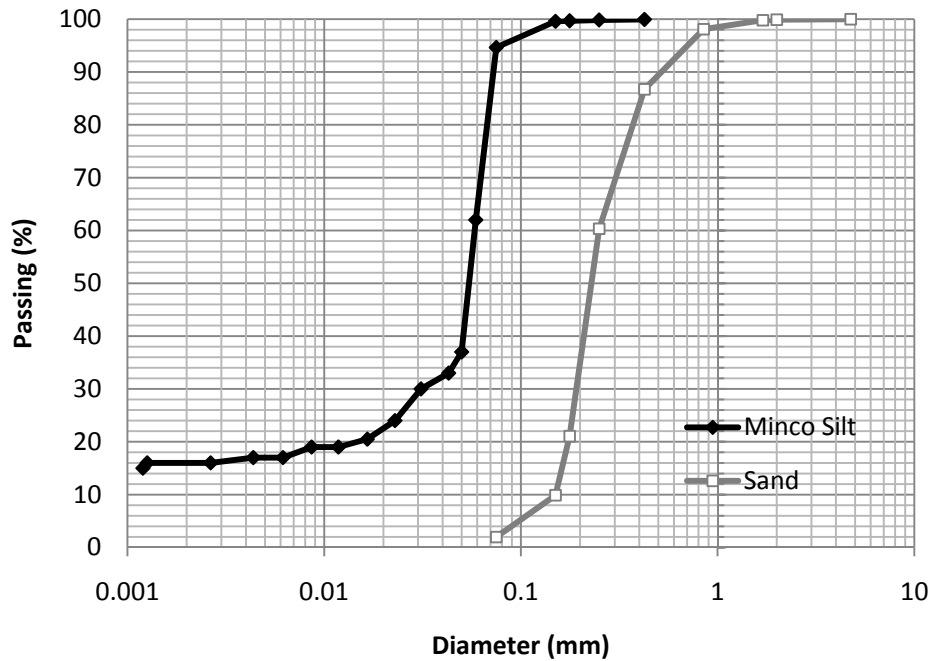


Figure 5. Gradation curves (sieve analysis) of sand and Minco silt

Table 2. Minco silt properties

<i>Minco silt (CL-ML)</i>	<i>Geary sample</i>	<i>Tan (2005)</i>
<i>Liquid Limit, %</i>	23	24
<i>Plastic Limit, %</i>	19	16
<i>Plasticity Index, %</i>	4	8
<i>Specific Gravity</i>	2.6	2.6
<i>Gravel, %</i>	0	0
<i>Sand, %</i>	29.7	23.2
<i>Fines, %</i>	70.3	76.8
<i>Maximum Dry Unit Weight, kN/m³ (pcf)</i>	17.2 (109.5)	18.1(115.2)
<i>Optimum Moisture Content, %</i>	12.7	13.6



Figure 6. Minco silt

The Soil-Water Characteristic Curve (SWCC) for Minco silt is given in **Figure 7**. It shows an inverse relationship between the soil water content (moisture content) and suction.

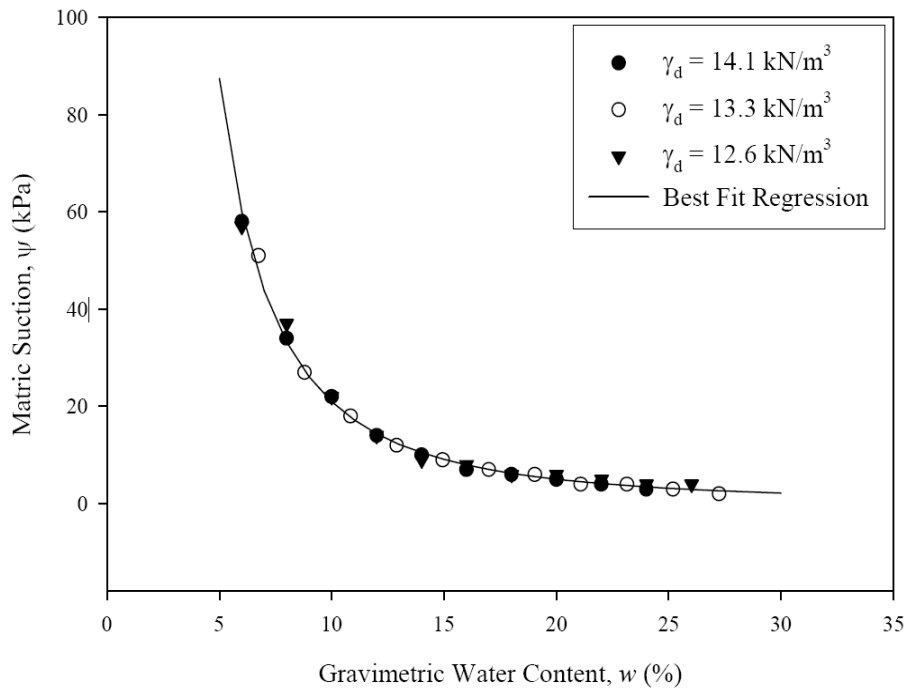


Figure 7. Soil-Water Characteristic Curve (SWCC) for Minco silt (Tan 2005)

The optimum moisture content and maximum dry unit weight of the Minco silt from standard Proctor tests were determined to be OMC = 12.7% and $\gamma_{dmax} = 17.2 \text{ kN/m}^3$ (109.5 pcf), respectively (**Figure 8**).

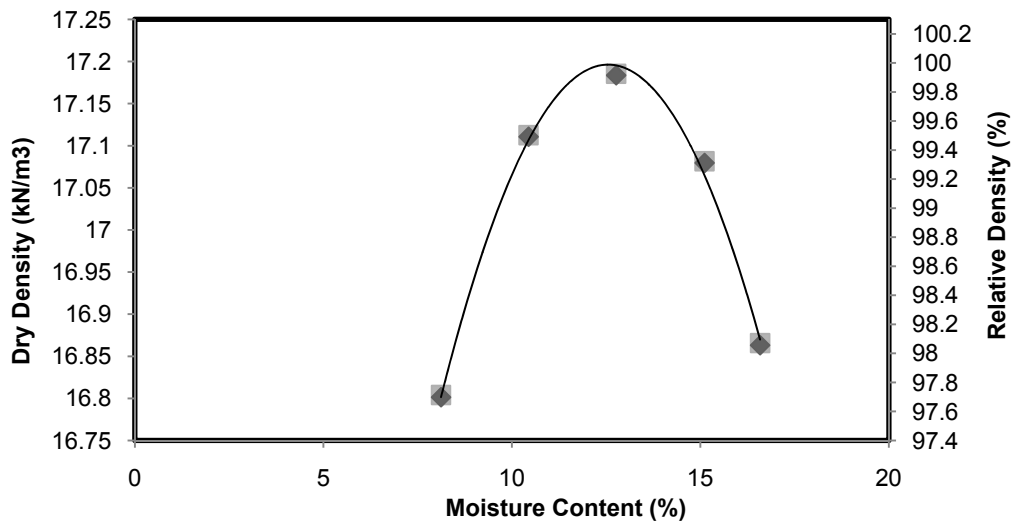


Figure 8. Standard Proctor test results on Minco silt

3.2. Geosynthetic Properties

A woven polypropylene (PP) geotextile (HP370) was used in the pullout tests carried out in this study (Figure 9). The mechanical response of the geotextile was found as per the ASTM D4595 test protocol (ASTM 2009) and it was compared with the manufacturer's data (Figure 10).



Figure 9. Geotextile (HP370)

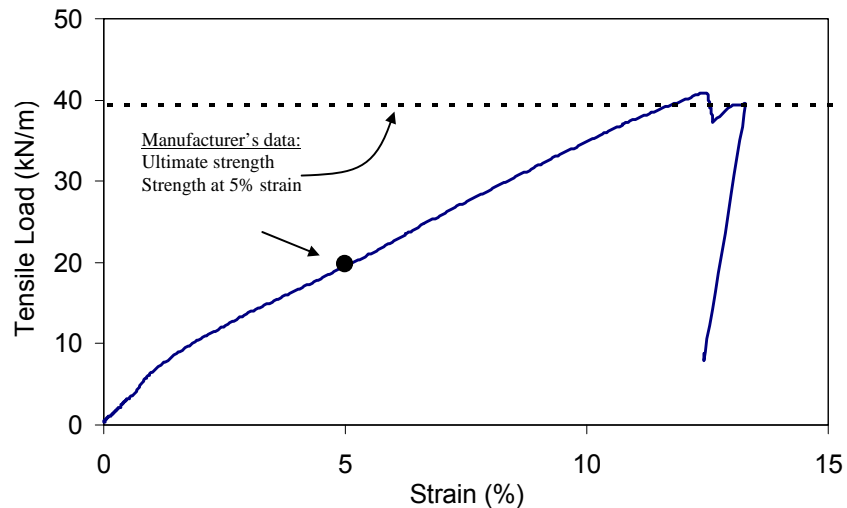


Figure 10. Mechanical response of geotextile (HP370) as per ASTM D4595 test protocol and as compared with the manufacturer's data

4. Large-Scale Pullout Tests

4.1. Methodology

A summary of the test conditions and material properties of the large-scale pullout tests is presented in the following table:

Table 3. Large-scale pullout test cases and material properties

<i>Test information</i>	<i>Uniformly graded fine sand (control set)</i>	<i>Minco silt (Sandy silt CL-ML)</i>
<i>Geosynthetic reinforcement</i>	TenCate HP370, woven PP	TenCate HP370, woven PP
<i>Overburden pressures, kPa (psi)</i>	3 (0.4), 8 (1.2), 10 (1.5), 20 (2.9), 50 (7.3), 68 (9.7)	10 (1.5), 20 (2.9), 50 (7.3)
<i>Moisture Content</i>	NMC ^(*)	OMC-2%; OMC; OMC+2%

^(*) NMC: Natural Moisture Content ($\omega = 0.6\%$)

A series of large-scale pullout tests were carried out in the uniformly graded fine sand (**Section 3**) to determine the pullout response and interface friction angle of the geotextile reinforcement in a good-quality soil as a reference point for tests on a marginal quality soil (i.e. Minco silt). The large-scale pullout tests on sand were carried out at six (6) different overburden pressures as given in **Tables 3 and 4**.

A second series of large-scale pullout tests were carried out in Minco silt and the same geotextile fabric (TenCate HP370, woven PP) (**Section 3**). These tests were carried out at three different moisture content values OMC-2%, OMC and OMC+2%. The differences in the geotextile pullout resistance among these cases with different moisture content values were used to determine a moisture reduction factor (MRF) in **Equation 1** to account for the loss of reinforcement pullout resistance due to increased moisture content. The tests for each moisture content value were carried out at three different overburden pressures (10 kPa, 20 kPa and 50 kPa).

4.1.1. Test Equipment

The nominal dimensions of the large-scale pullout test box (**Figure 11**) are 1800 mm (L) x 900 mm (W) x 750 mm (H). The size of the box and its basic components, including

metal sleeves at the front end well exceed the requirements of the ASTM D6706 test protocol (ASTM 2009). The boundary effects were further minimized by lining the walls of the test box with plastic sheets. The test box also has a $\frac{3}{4}$ "-thick plexiglass transparent panel wall on one side to allow for visual observation of the soil deformation and soil-interface performance over the course of pullout testing. The large pullout test equipment has a 4" bore, 18" stroke hydraulic cylinder with a high precision servo-control system. A surcharge assembly including an airbag and reaction beams on the top of the soil surface is used to apply overburden pressures up to about 50 kPa (i.e. approximately 7 psi, or equivalent to 3 m of overburden soil). The pullout load on the reinforcement specimen was applied using a 90 kN (20 kip), servo-controlled hydraulic actuator. In the tests carried out in this study, only half of the box length (i.e. 900 mm) was used.

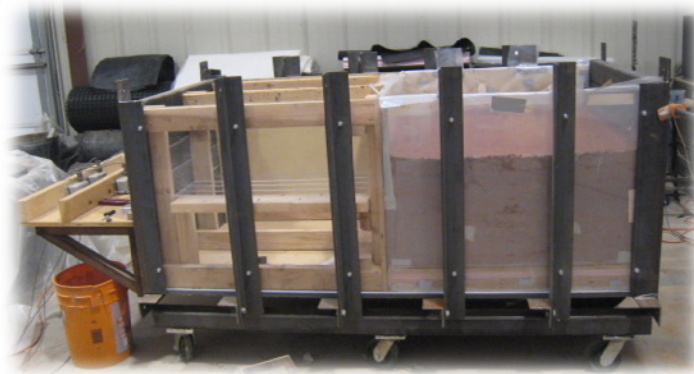


Figure 11. Pullout test box

4.1.2. Instrumentation

Different instruments were used to measure the matric suction and moisture content in the soil, especially near the soil-reinforcement interface. A set of tensiometer probes was placed in rows above and below the soil-geotextile interface (**Figure 12**).

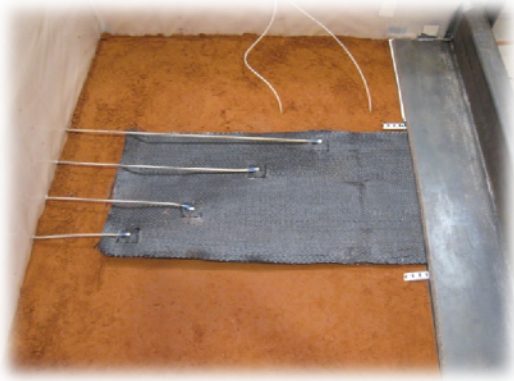


Figure 12. (a) Tensiometer probes placed near the soil-geotextile interface, (b) tensiometer readout dials

The geotextile strains and local displacements were measured using four (4) wire-line extensometers attached to different locations along the reinforcement length (**Figure 13a**). A Geokon Earth Pressure Cell (EPC) was used to verify the magnitude of the overburden pressure applied by the airbag on the interface. Geokon Earth Pressure Cells (**Figure 13b**) use vibrating wire pressure transducers and thus have the advantages of long term stability, reliable performance with long cables and insensitivity to moisture intrusion.

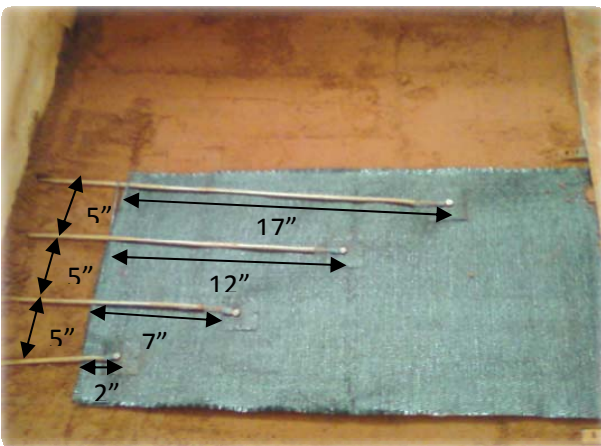


Figure 13. (a) wire-line extensometers attached to the geotextile reinforcement (b) earth pressure cell placed at the top of the soil in the pullout test box

4.2. Large Scale Pullout Tests in Sand

The large-scale pullout tests involved careful placement and compaction of a significant amount of sand. First, the pullout box was lined with plastic sheets to minimize friction between the soil and sidewalls during testing. Next, sand was placed and compacted in two-inch soil lifts. Preliminary pullout tests were carried out to determine a minimum suitable thickness of the soil above and below the interface (see the discussion on **Table 4** below).

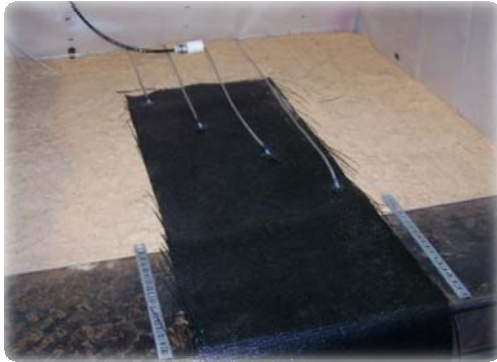


Figure 14. HP 370 Geotextile placed at the middle of the pullout box with wireline extensometers attached



Figure 15. A sideview of the soil and filler panels in the pullout box



Figure 16. Placement of earth pressure cell on the top of soil in the test box



Figure 17. A sideview of the pullout test box filled with soil

Two (2) tests were carried out with 150 mm (6") of sand above and below the geotextile fabric in which the soil was compacted to 93% relative density at its natural moisture content ($\omega = 0.6\%$). Six (6) additional tests were carried out using 200 mm (8") of sand above and below the geotextile fabric (**Figures 14 through 16**) and the same relative

density and moisture content. Afterwards, an earth pressure cell was placed on the top of the sand (**Figure 17**) to measure the normal stress applied on the soil using an air bag. Finally, the pullout box was sealed and the geotextile fabric was attached to the actuator. The actuator displacement rate was 1 mm/min. The duration of the pullout test varied between 45 and 60 minutes depending on the level of normal stress applied to the interface. **Table 4** provides a summary of the large-scale pullout test conditions in the sand.

Table 4. Large-scale pullout tests in sand

<i>Test information</i>	<i>Test 1*</i>	<i>Test 2*</i>	<i>Test 3</i>	<i>Test 4</i>	<i>Test 5</i>	<i>Test 7</i>	<i>Test 8</i>	<i>Test 9*</i>
<i>Overburden pressure on the interface, kPa (psi)</i>	8 (1.2)	8 (1.2)	8 (1.2)	3 (0.4)	10 (1.5)	20 (2.9)	50 (7.3)	68 (9.7)
<i>Soil thickness below and above geosynthetic, mm (in)</i>	150 (6)	150 (6)	200 (8)	200 (8)	200 (8)	200 (8)	200 (8)	200 (8)
<i>Moisture content (%)</i>	0.5	0.6	0.6	0.6	0.6	0.6	0.6	0.5

*Note: *Not included in final calculations of interface friction angle.*

According to the ASTM D6706 test protocol, the reinforcement specimens should be horizontally embedded between two, 150-mm (6-inch) layers of soil. However, it was decided to compare the pullout response of the geosynthetic specimen when placed in 150 mm (6") and 200 mm (8") of soil below and above it to determine whether a larger amount of soil would be required to minimize boundary effects in the tests. Therefore, Tests 2 and 3 were nominally identical (e.g. with respect to the materials, soil unit weight, overburden pressure at the interface level, loading rate, etc.) with the exception of the thickness of soil between the geosynthetic and the upper and lower solid boundaries. The two test results were similar which is illustrated in **Figure 18**. However, to accommodate tensiometers, which were used to monitor soil moisture and suction levels, it was decided to place 200 mm (8") of soil above and below the geotextile. The additional soil also further mitigated any boundary effects.

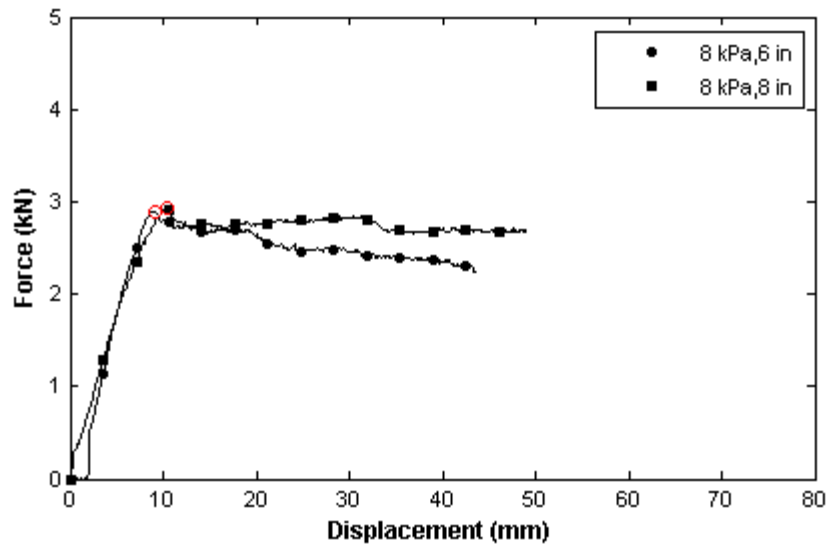


Figure 18. Comparison of load-displacement responses of geotextile reinforcement embedded in 6'' and 8'' of sand (Tests 2 and 3)

4.2.1. Interface friction angle

Pullout test data for Tests 3 through 9 are shown in **Figure 19**. These results show a consistent trend with respect to the influence of overburden pressure on the pullout peak load and performance. Lower overburden pressure values (e.g. less than 50 kPa) represent more critical cases for pullout resistance in reinforced soil walls and embankments.

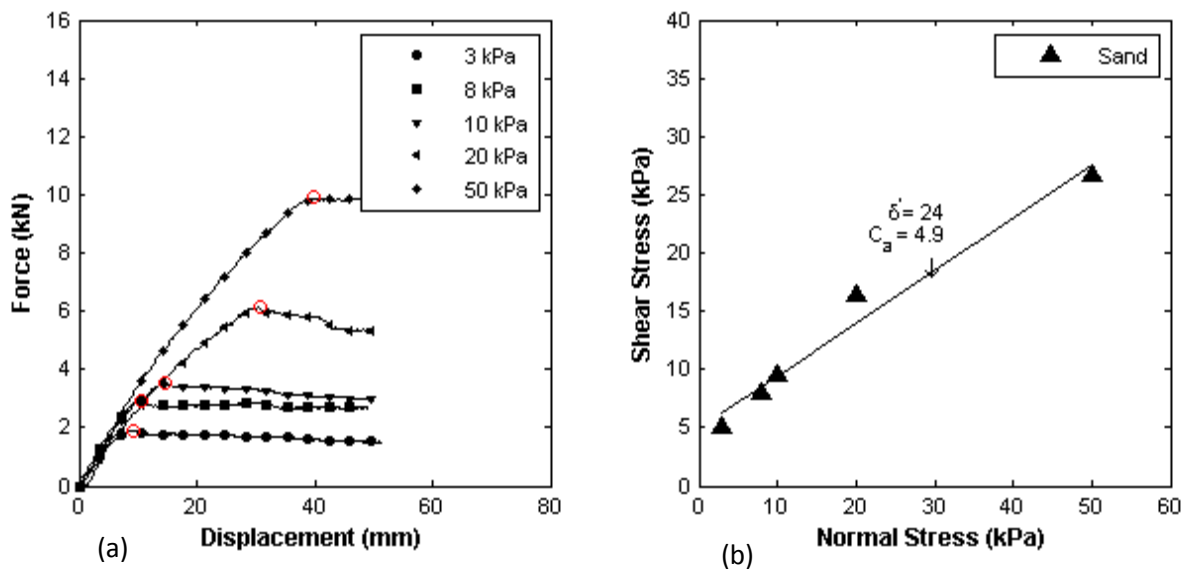


Figure 19. (a) Pullout test results on HP370 woven geotextile embedded in 200 mm (8") sand (b) overburden stress vs. pullout resistance

Table 5. Pullout test results (200 mm soil embedment cases)

$w.c$ (%)	σ_n kPa (psi)	P_r kN (lb)	τ_{max} kPa (psi)	$\delta^{(1)}$ degrees	C_a kPa ⁽¹⁾ (psi)
0.6 (NMC)	3 (0.4)	1.9 (429.6)	5.1 (0.8)	24	4.9 (0.8)
	8 (1.2)	2.9 (661.0)	7.9 (1.2)		
	10 (1.4)	3.5 (791.1)	9.5 (1.4)		
	20 (2.9)	6.1 (1376.2)	16.5 (2.4)		
	50 (7.3)	9.9 (2223.2)	26.6 (3.9)		

Notes: (1) from maximum pullout resistance (P_r)

Figure 20 shows photographs of geotextile specimens at the end of pullout tests at different overburden pressure magnitudes as follows: (a) under 68 kPa overburden pressure, the geotextile failed at 10.47 kN (prior to peak pullout resistance) close to the roller connection outside the soil (**Figure 21**); (b) under 53 kPa overburden pressure, the geotextile failed inside the metal sleeves inside the test box after reaching the maximum pullout resistance; (c) for cases with overburden pressure equal to 10 kPa or less, the geotextile pulled out without any rupture.

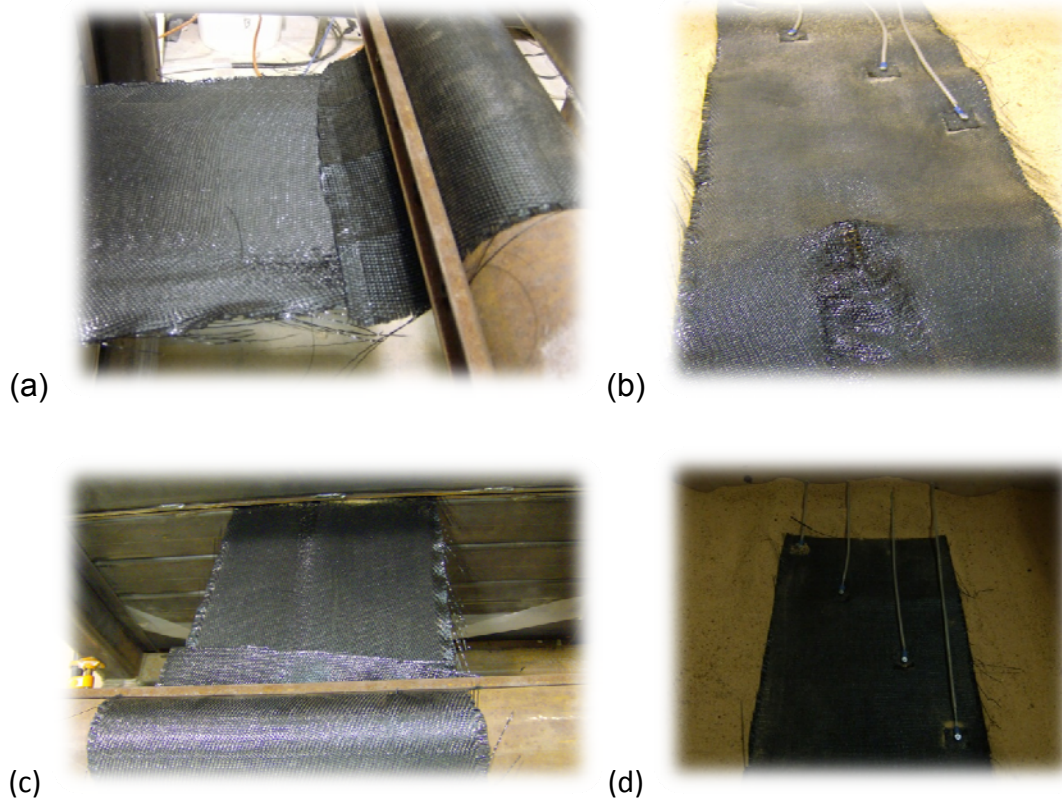


Figure 20. (a-c) Mechanical performance of the PP woven geotextile when pulled out under different overburden pressure magnitudes: (a) 68 kPa, (b) 50 kPa, (c) 10 kPa; (d) locations of telltales (extensometers) on the geotextile specimens

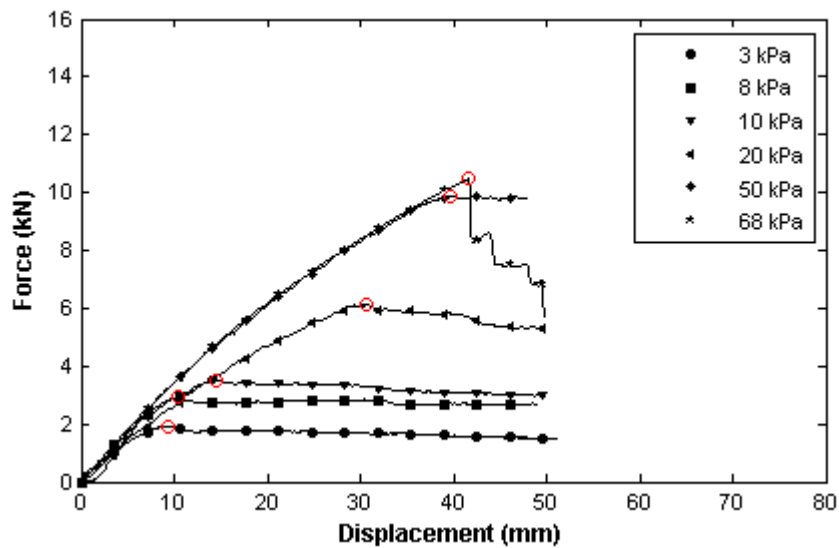


Figure 21. Pullout test results on HP370 woven geotextile embedded in 200 mm (8'') sand including test 9 (peak pullout loads are marked with hollow circles)

As opposed to pullout resistance, reinforcement rupture becomes the dominant failure mode for greater overburden pressure magnitudes as evidenced by the rupture of the reinforcement prior to complete pullout in the 68 kPa case shown in **Figure 21**. The interface friction angle from the results shown in **Figure 19** was determined to be $\delta' = 24^\circ$ which is the same values for uniform fine sand and woven geotextiles reported in the literature for concrete sand (Koerner 2005).

Having obtained satisfactory results from our pullout tests in sand, we began our second series of tests in Minco silt with the focus on the influence of moisture content on the pullout resistance of geosynthetic reinforcement in marginal soils.

4.3. Large-Scale Pullout Tests in Minco Silt

After the soil was transported from the borrow site to the Fears lab, the soil was dried to its natural moisture content of 0.4%, and then it was passed through the #4 sieve **Figure 22**. The coarser particles and chunks were taken to the Broce lab and grinded and sieved again through the #4 sieve. Then the soil was mixed with water to reach the desired moisture content for each test. Mixing of the soil took approximately 5 hours (**Figures 23 through 25**). The wet soil was stored in thirty three 25 kg (55 lb)-buckets and sealed for more than 24 hours to reach internal equilibrium. The soil moisture content in each bucket was measured using the oven drying method.



Figure 22. Mixing of Minco silt with water



Figure 23. Sieving processes



Figure 24. Soil samples in the oven (one sample per bucket) to determine their moisture content



Figure 25. Minco silt in 33 sealed buckets

The pullout box was lined with plastic sheets (**Figures 26 and 27**) to preserve the soil moisture content and to minimize the friction between the soil and the sidewalls during testing. Next, the soil was placed and compacted in the test box in eight two-inch lifts.

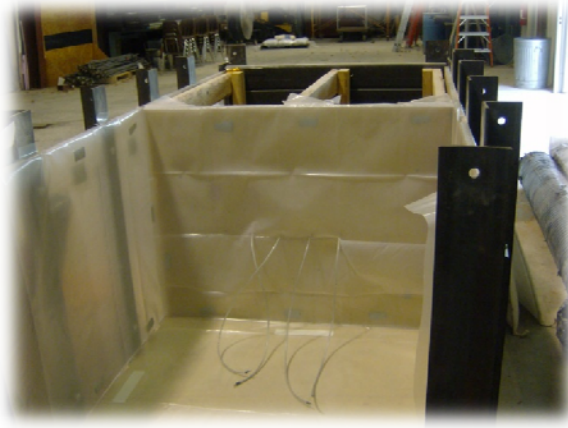


Figure 26. Pullout box lined with plastic sheets

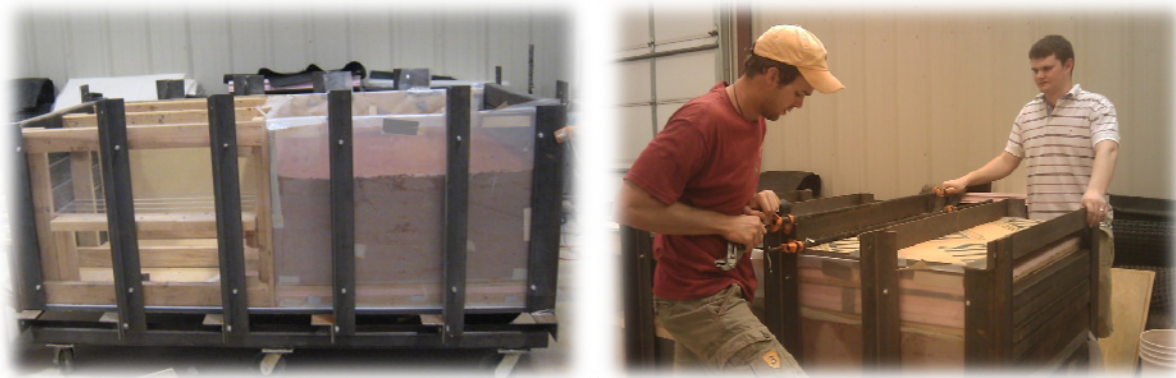


Figure 27. Pullout box set up

Compacting Minco silt in the box to 93% of its maximum dry unit weight was found to be challenging. As a result, the soil was compacted to 86% of its maximum dry unit weight (i.e. $\gamma_d = 14.81 \text{ kN/m}^3 = 94.3 \text{ pcf}$), with a corresponding bulk unit weight of $\gamma = 16.40 \text{ kN/m}^3$ (104.4 pcf). The soil target unit weight in the test box was reached using volumetric control compaction. The compaction for each layer took approximately 45 minutes. The instrumented geotextile and the tensiometers were placed at the mid-height of the box as shown in **Figure 28**. The placement of the tensiometer and the geotextile took between one hour and half approximately. The pullout box containing compacted Minco silt at its target moisture content was sealed with plastic sheets on the top (**Figure 27**). The soil was monitored for 4 - 5 days until the tensiometers all reached equilibrium and showed constant readings.

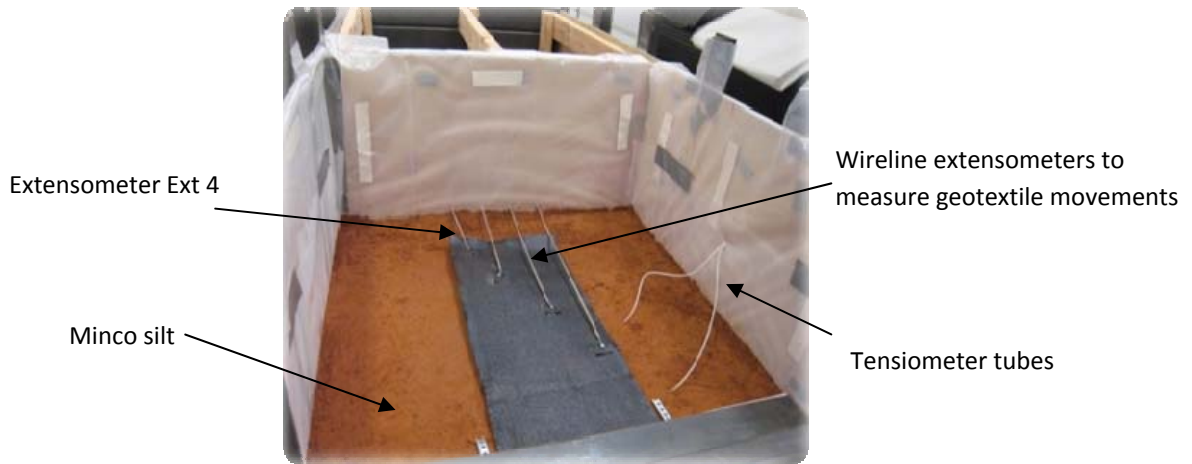
The pullout phase of the test usually took between 40 minutes and 1.5 hours depending

on the overburden pressure. After the test was completed and the reinforcement underwent pullout failure, the test assembly was carefully dismantled. First, the surcharge assembly was removed from the top of the box. The exposed soil was examined for any sign of cracking or other movement, followed by careful excavation. It usually took about 5 to 7 hours to carefully dig the entire soil out of the test box. All together, a complete test required approximately 24 hours of hands-on preparation, 5 to 6 days of observation and monitoring, and 2/3 to 3/2 hours to run the pullout test.

Table 6. Test information for large-scale pullout tests

<i>Test information</i> ⁽¹⁻³⁾	<i>Test 1</i>	<i>Test 2</i>	<i>Test 4</i>	<i>Test 5</i>	<i>Test 6</i>	<i>Test 7</i>	<i>Test 8</i>	<i>Test 9</i>	<i>Test 10</i>
	<i>OMC-2%</i>	<i>OMC-2%</i>	<i>OMC-2%</i>	<i>OMC</i>	<i>OMC</i>	<i>OMC</i>	<i>OMC+2%</i>	<i>OMC+2%</i>	<i>OMC+2%</i>
<i>Target σ_n on the interface, kPa (psi)</i>	10 (1.5)	20 (2.9)	50 (7.3)	10 (1.5)	20 (2.9)	50 (7.3)	10 (1.5)	20 (2.9)	50 (7.3)
<i>Target ω. (%)⁽⁴⁾</i>	10.7	10.7	10.7	12.7	12.7	12.7	14.7	14.7	14.7
<i>Measured ω. (average) (%)⁽⁵⁾</i>	10.8	10.4	10.8	12.5	12.6	12.5	14.8	14.6	14.7
<i>Anticipated ψ kPa (psi)⁽⁶⁾</i>	18 (2.6)	18 (2.6)	18 (2.6)	12 (1.7)	12 (1.7)	12 (1.7)	10 (1.5)	10 (1.5)	10 (1.5)
<i>Measured ψ (average) kPa (psi)</i>	31 (4.5)	31 (4.5)	18.4 (2.7)	24.6 (3.6)	24.5 (3.6)	24.6 (3.6)	13 (1.9)	12 (1.7)	13.1 (1.9)

Notes: (1) All tests were carried out in Minco silt, (2) Soil thickness below and above the geosynthetic is 200 mm (8 inches), (3) Geosynthetic reinforcement in all tests is TenCate HP370 PP woven geotextile, (4) OMC for Minco Silt is 12.7%, (5) see **Figure 31** for locations of MC measurements; the average value is calculated over the soil-geotextile interface only, (6) from **Figure 7** and using the measured average moisture content values.



(a)

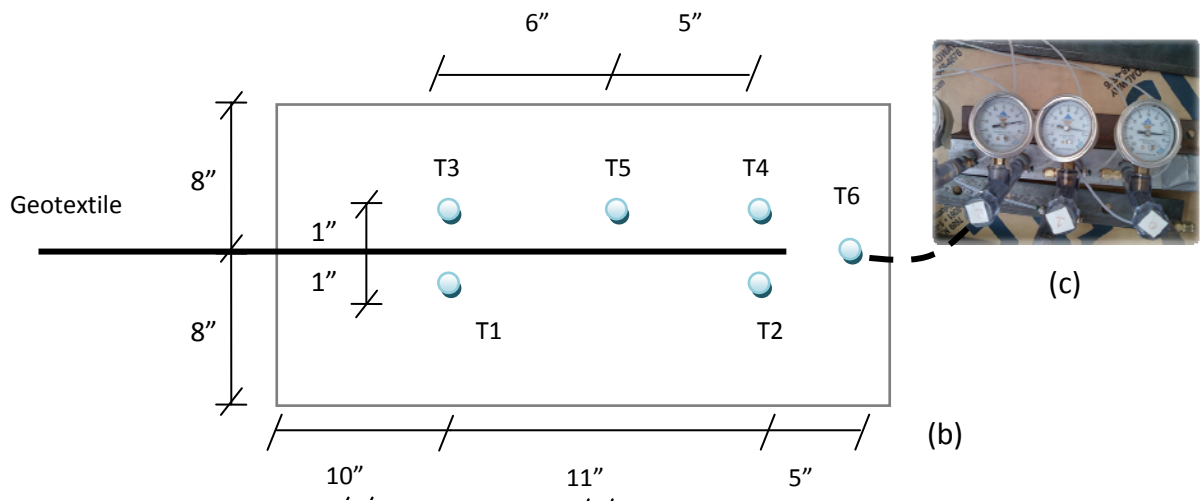


Figure 28.(a) Tensiometer probes placed near the soil-geotextile interface and wire-line extensometers attached to geotextile; (b) schematic diagram indicating the locations of tensiometers in the pullout test box; (c) tensiometer dial gauges

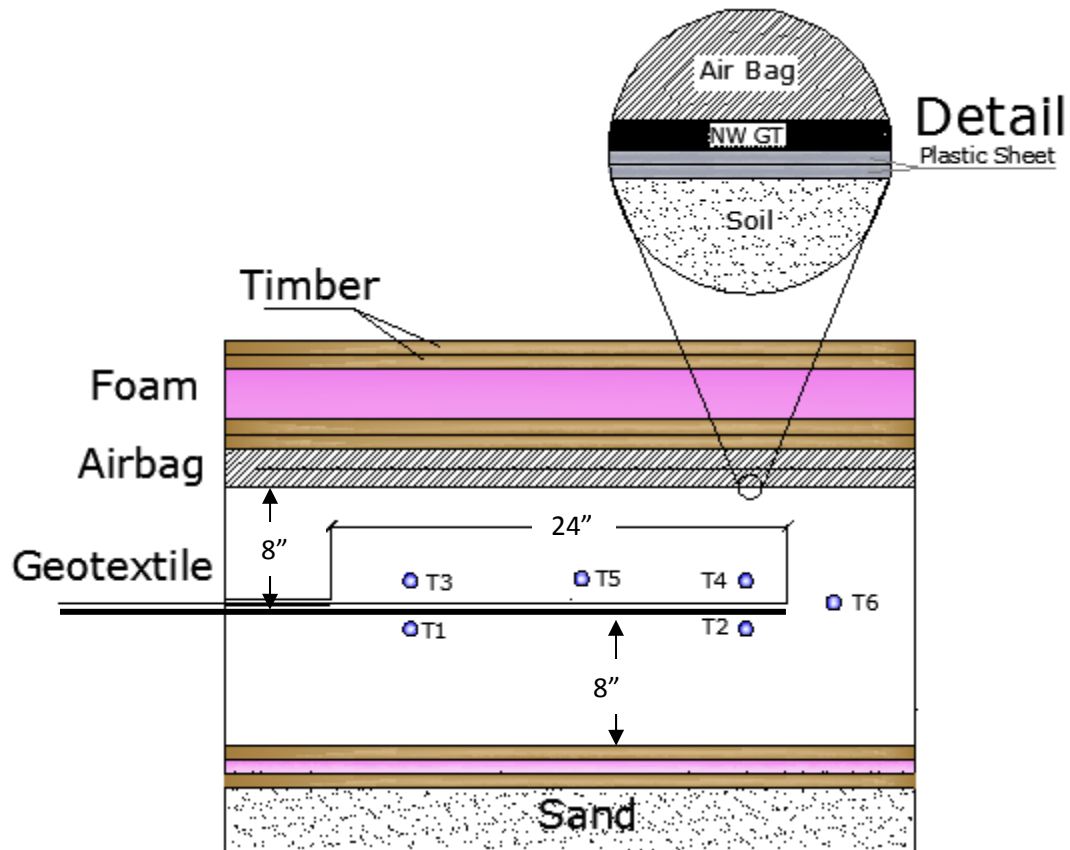


Figure 29. Schematic diagram of the pullout box

The soil was both compacted and excavated in the test box in eight 50.8 mm (2")-layers. Sample of water content were taken in each layer before and after all tests (Figure 30). The moisture content (ω) in layers 5 through 8 were taken from Region 1 and the moisture content in layers 1 through 4 were taken from Region 2 as shown in Figure 31. Layers 1 and 8 represent the bottom layer and the top layer, respectively.

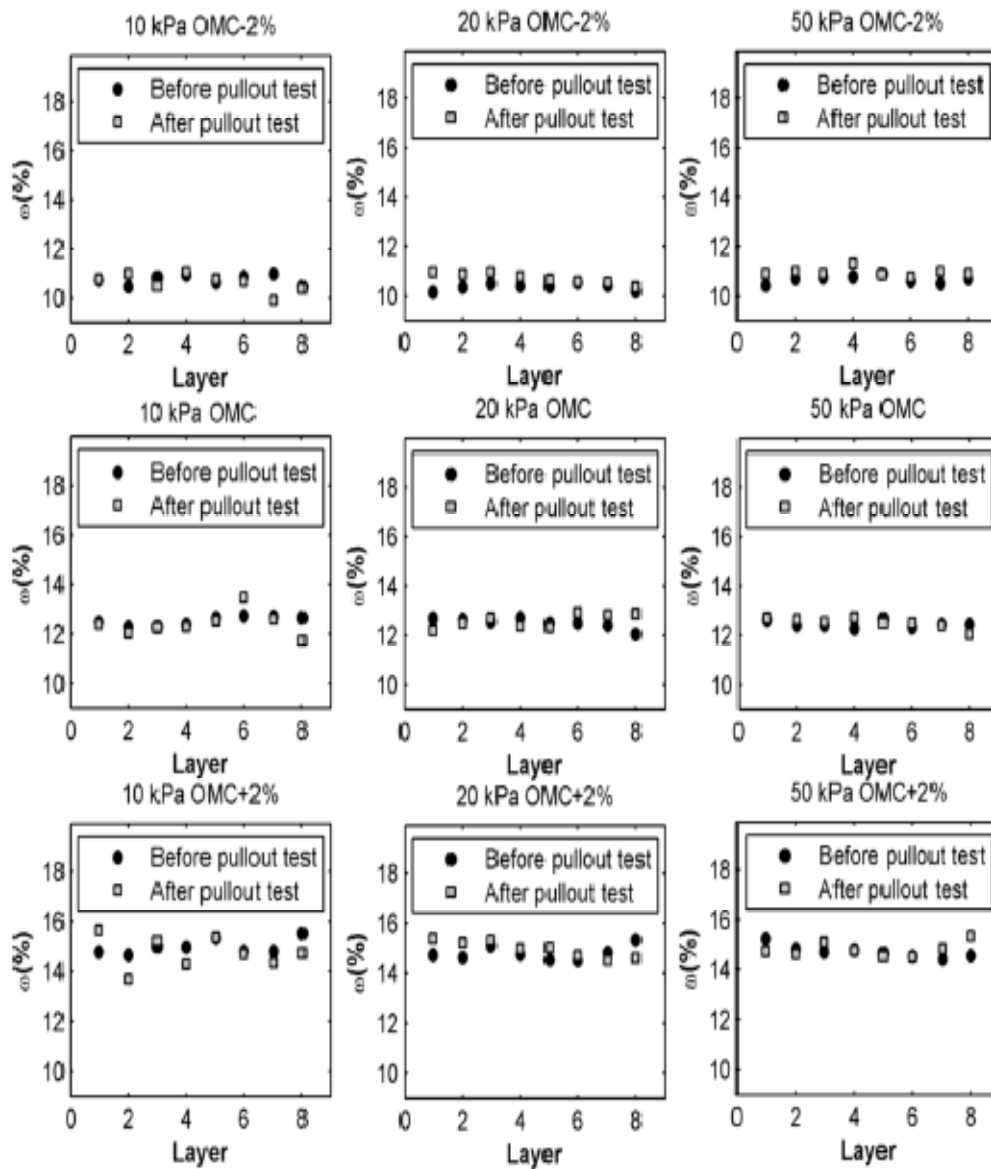


Figure 30. Moisture content within each layer inside the pullout box at OMC-2%, OMC and OMC+2% for each test

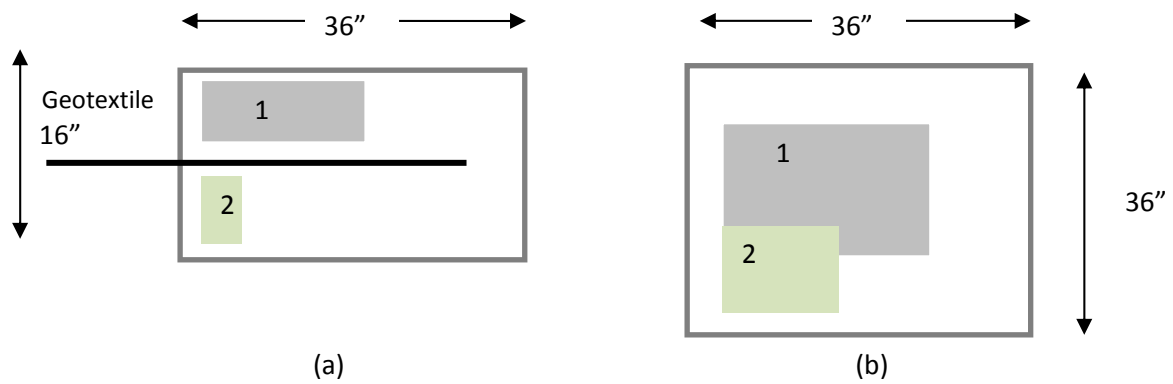


Figure 31. Regions within the test box where soil samples were taken to measure moisture content, (a) side view, (b) plan view

4.3.1. Interface friction angle

Pullout test data for Minco silt at *nominal* moisture content values OMC-2% (10.7%), OMC (12.7%) and OMC+2% (14.7%) are shown in **Figure 32**. The measured pullout force is plotted as a function pullout displacement. Results shown in **Figure 32** show that the reinforcement pullout resistance is greater for greater overburden pressure (or normal stress, σ_n) magnitudes. **Figures 32** shows consistently higher maximum reinforcement pullout resistances at OMC-2% compared to the values in the OMC and OMC+2% cases for overburden pressure magnitudes of 10 kPa, 20 kPa and 50 kPa. As expected, increasing suction led to higher maximum reinforcement pullout resistances in identical test specimens (**Figures 32d**).

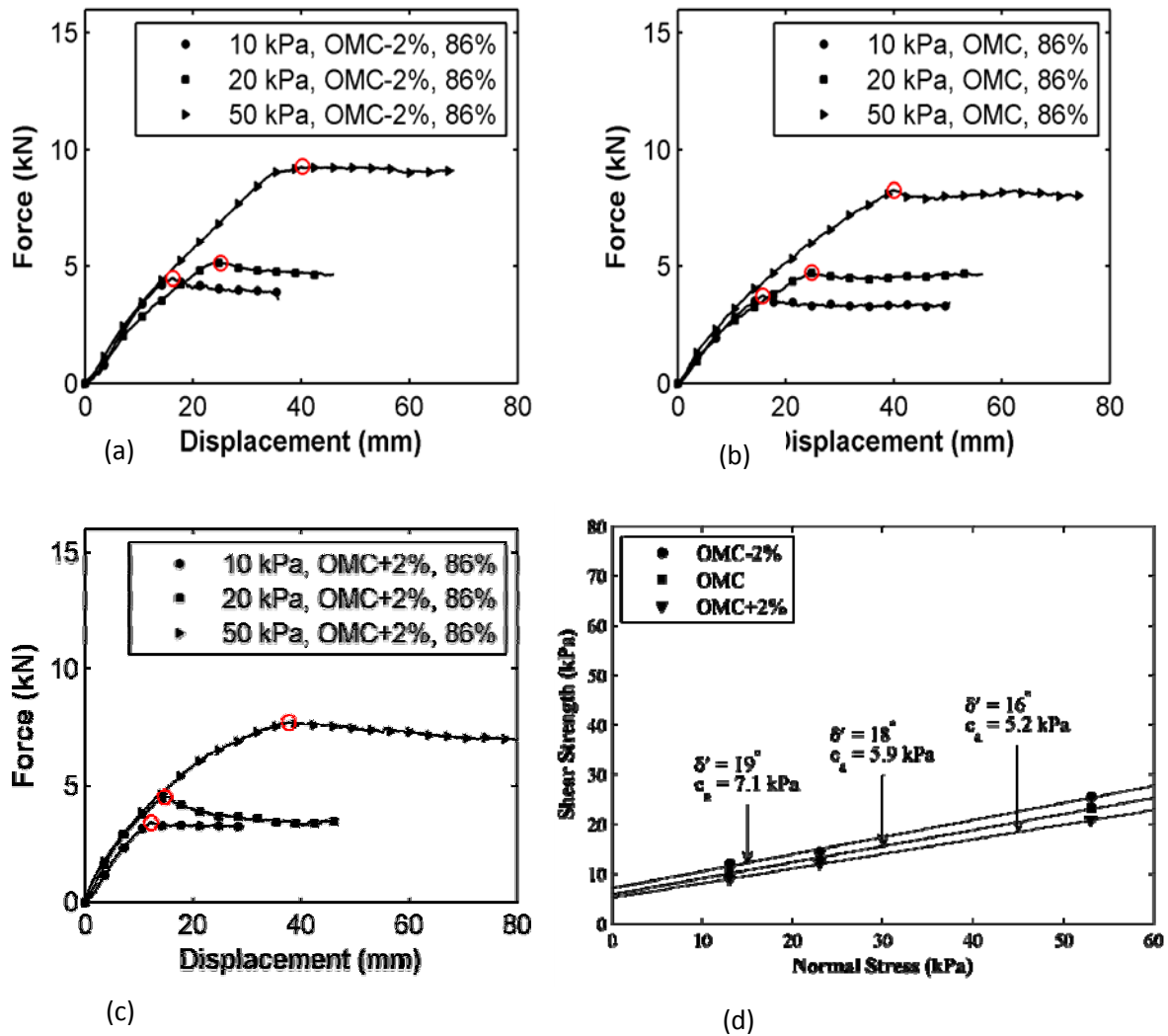


Figure 32. Pullout test data for Minco silt and interface strength results for Minco silt and comparison of failure envelopes for soil-geotextile Interface at different moisture contents (OMC-2%, OMC and OMC+2%).

The interface strength results for the geotextile reinforcement in Minco silt are shown in **Figure 32d** and summarized in **Table 7**. The interface strength values correspond to the maximum pullout resistance (P_r) values shown in **Figure 32**. We believe that any further increase in the observed pullout force beyond the point shown in each graph in **Figure 32** is merely due to the test condition (e.g. strain-hardening due to jamming of the soil within the gap between the sleeves) and is of little practical significance.

Table 7. Interface strength properties from pullout tests in Minco silt

Target $\omega^{(2)}$ %	σ_n kPa (psi)	Average ω (%) ⁽¹⁾	Average ψ (kPa) ⁽³⁾	P_r kN (lb)	τ_{max} kPa (psi)	$\delta^{(4)}$ ($^\circ$)	C_a (kPa) ⁽⁵⁾
10.7 (OMC-2%)	10 (1.4)	10.8	31.0	4.5 (1004.1)	12.1 (1.8)	19	7.1
	20 (2.9)	10.4	31.6	5.2 (1164.8)	14.0 (2.0)		
	50 (7.3)	10.8	30.3	9.3 (2086.7)	25.0 (3.6)		
12.7 (OMC)	10 (1.4)	12.5	24.6	3.7 (842.9)	10.1 (1.5)	18	5.9
	20 (2.9)	12.6	24.5	4.7 (1058.7)	12.7 (1.8)		
	50 (7.3)	12.5	24.6	8.3 (1864.3)	22.3 (3.2)		
14.7 (OMC+ 2%)	10 (1.4)	14.8	13.4	3.4 (761.3)	9.1 (1.3)	16	5.2
	20 (2.9)	14.6	11.8	4.5 (1011.8)	12.1 (1.8)		
	50 (7.3)	14.7	13.1	7.7 (1741.0)	20.8 (3.0)		

Notes: (1) Target moisture content (ω) with variations of OMC \pm 2%, (2) The average moisture content (ω) value calculated over soil-geotextile interface layers 4 and 5 only, (3) average of suction (ψ) obtained from the tensiometers, (4,5) from maximum pullout resistance (P_r).

The results shown in **Figure 32** represent the frontal planes of the extended Mohr-Coulomb failure envelopes for the soil-geotextile interface at different moisture content and suction values. The resulting values can be considered to be practically linear for all the cases OMC-2%, OMC and OMC+2%. The slope and the intercept of the failure envelopes on these frontal planes are referred to δ' , and c_a , respectively (**Table 7**).

4.3.2. Soil moisture content and suction

Figure 33 shows the soil suction data during pullout tests at OMC-2%, OMC, and OMC+2%. The data do not indicate any clear dependence of the soil suction on the overburden pressure or pullout displacement. However, it was noticed that the suction

measurements from the tensiometers were sensitive to the elevation of their readout cylinder during the test. As notice in 50 kPa at OMC-2% test, the tensiometer cylinders were at a lower elevation from the rest of the tests. In pullout tests at OMC and OMC+2% the tensiometers readout cylinders were kept at the same elevation across different tests with different overburden pressures. As a result, the suction data in **Figure 33** for the tests carried out at OMC and OMC+2% under different confining pressure values are comparable.

Pullout test data for Minco silt at 10 kPa, 20 kPa and 50 kPa overburden pressure, varying suction and moisture content are shown in **Figure 34**. The measured pullout force is plotted as a function of pullout displacement. The interface strength results for the geotextile reinforcement in Minco silt are also shown in **Figure 34** and summarized in **Table 8**. The interface strength values in **Table 8** correspond to the maximum pullout resistance (P_r) values shown in **Figure 34**.

Results shown in **Table 8 and Figure 34** show slightly (and consistently) higher maximum reinforcement pullout resistances at OMC-2% than for OMC and OMC+2% for overburden pressure values of 10 kPa, 20 kPa and 50 kPa.

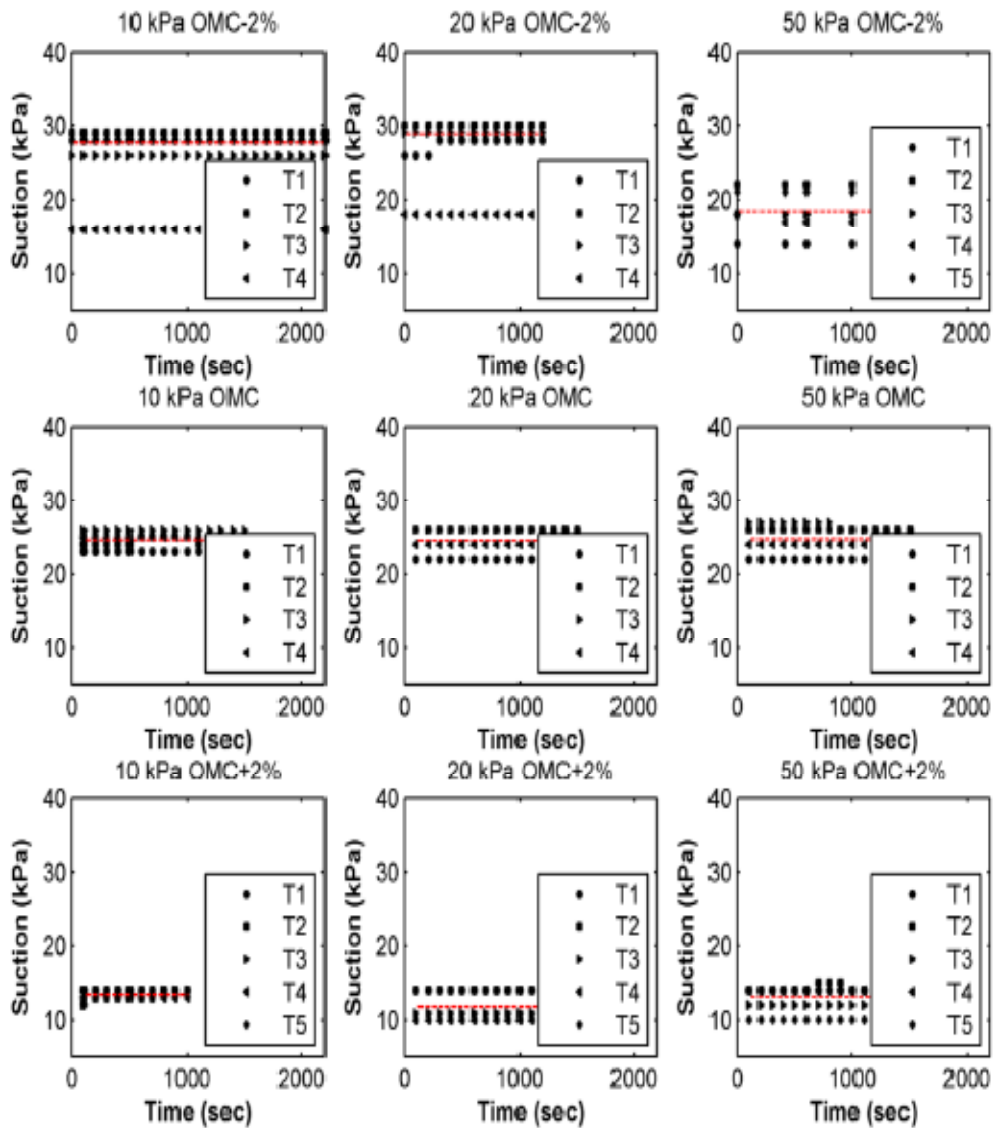


Figure 33. Suction data for pullout tests in Minco silt, the horizontal line in each graph indicates the average suction value from Table 6.

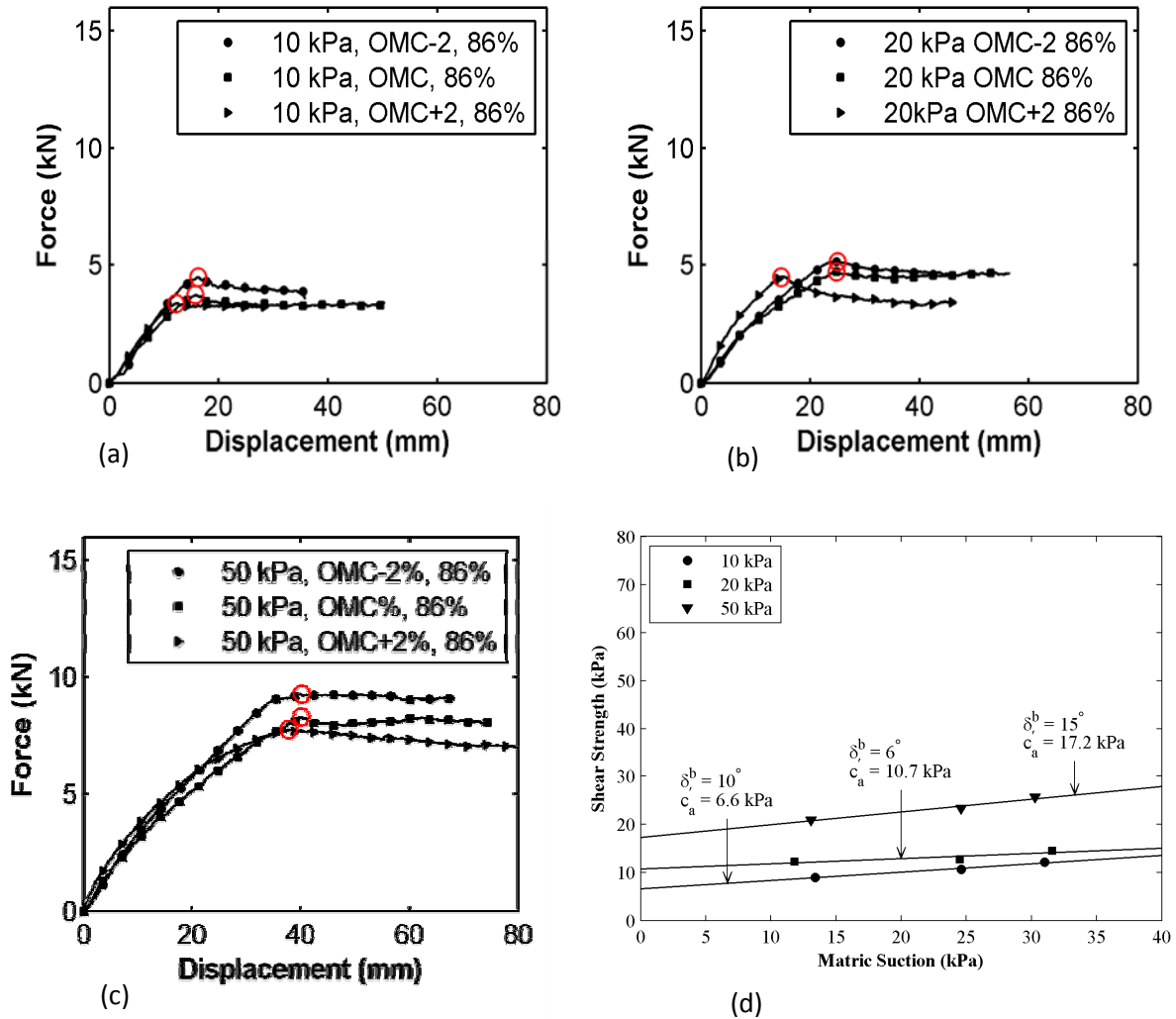


Figure 34. Data for large-scale pullout tests in Minco Silt and comparison of failure envelopes of the soil-geotextile interface for determination of effective adhesion (c_a') and friction angle (δ^b) between soil and geotextile interface at different suctions

Table 8. Interface strength properties from pullout tests in Minco silt as a function of suction

σ_n kPa (psi)	Average ω (%) ⁽¹⁾	Average ψ (kPa) ⁽²⁾	P_r kN (lb)	τ_{max} kPa (psi)	δ^b ⁽⁴⁾ ($^\circ$)	C'_a (kPa) ⁽⁵⁾
	10.8	31.0(4.5)	4.5 (1004.1)	12.1 (1.8)		
10 (1.4)	12.5	24.6 (3.6)	3.7 (842.9)	10.1 (1.5)	10	6.4
	14.8	13.4 (1.9)	3.4 (761.3)	9.1 (1.3)		
	10.4	31.6(4.6)	5.2 (1164.8)	14.0 (2.0)		
20 (2.9)	12.6	24.5 (3.6)	4.7 (1058.7)	12.7 (1.8)	6	10.7
	14.6	11.8 (1.7)	4.5 (1011.8)	12.1 (1.8)		
	10.8	30.3 (4.4) ⁽³⁾	9.3 (2086.7)	25.0 (3.6)		
50 (7.3)	12.5	24.6 (3.6)	8.3 (1864.3)	22.3 (3.2)	15	12.5
	14.7	13.1(1.9)	7.7 (1741.0)	20.8 (3.0)		

Notes: (1) The average moisture content (ω) value calculated over soil-geotextile interface layers 4 and 5 only, (2) average of suction (ψ) obtained from the tensiometers, (3) suction values from tensiometers when their readout cylinders were placed at a different elevation compared to the other tests, (4,5) from maximum pullout resistance (P_r).

The results shown in **Figure 34** represent the lateral planes of the 3D extended Mohr-Coulomb failure envelopes for the soil-geotextile interface as a function of suction. The line intercept and slope ω represent the effective adhesion equal to zero normal stress ($\sigma_n = 0$ kPa), and interface friction angle with respect to suction (δ^b), respectively. **Figure 35** shows the frontal and lateral failure envelopes of the extended Mohr-Coulomb envelopes for the soil-geotextile interaction at different normal stress (σ_n) and suction (ψ) values.

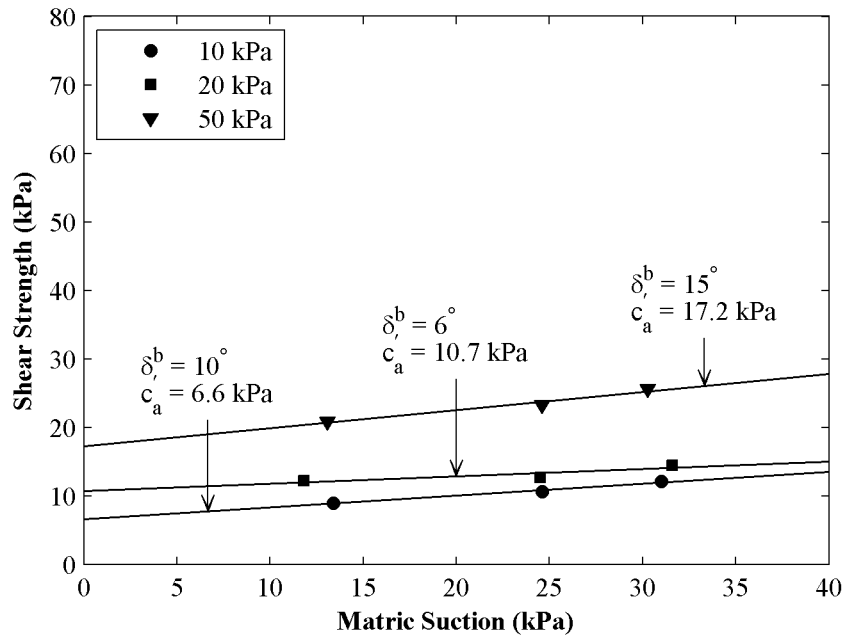
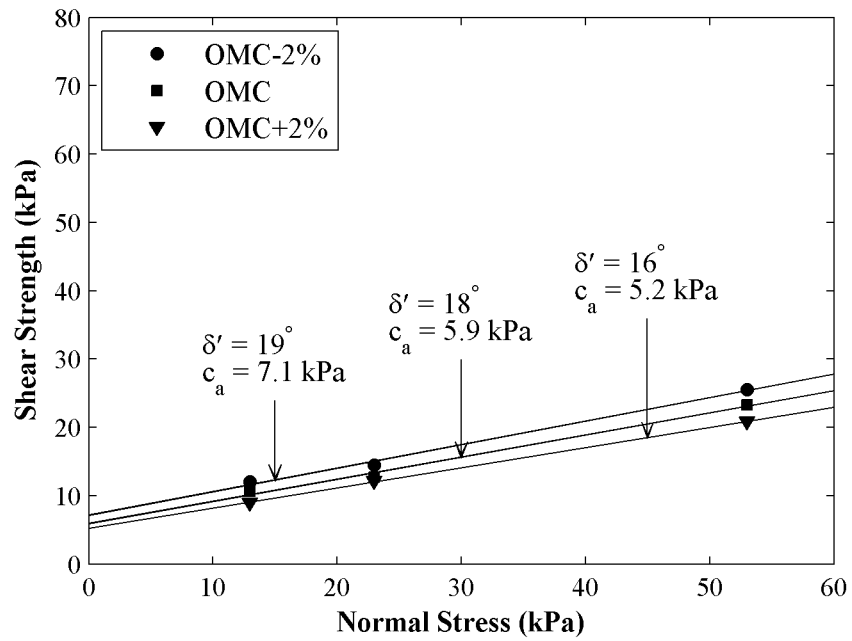


Figure 35. Extended Mohr-Coulomb failure envelopes for the soil-geotextile interface

4.3.3. Parameters α and F^*

Large-scale pullout tests in Minco silt were used to obtain pullout parameters for the geotextile reinforcement including the values for α and F^* in **Equation 1**. The correction factor α depends on the reinforcement extensibility and length. The parameter $F^* = \tan \delta_{peak}$ includes the contributions of both passive and frictional resistance components in the reinforcement pullout resistance.

Example calculations according to the FHWA (Elias et al. 2001) recommended method to determinate α are shown in **Figure 36**. First, the measured pullout force is plotted as a function of pullout displacement. Second, the normalized pullout displacement is plotted versus mobilized reinforcement length, L_p . Different mobilized lengths are obtained from four wire extensimeters attached to the geotextile reinforcement surface. Third, the value of P_r for each confining pressure magnitude (σ_v) is plotted versus $\sigma_v L_p$ from which the values for F_{peak} and F_m are determined. Finally, the correction factor α is plotted versus L_p . The calculated value of the correction factor for our pullout tests in Minco Silt from **Figure 36** is 0.55. This value is in a close agreement with $\alpha = 0.6$ as recommended by FHWA (Elias et al. 2001) for geotextiles.

Table 9. Large-scale pullout test in Minco to obtain values for α and F^*

Target $\omega^{(2)}$ %	σ_n kPa (psi)	P_r kN (lb)	T_{peak} kPa (psi)	α	$F^* = \tau_{peak}/\sigma_n$
	10 (1.4)	3.1 (690.5)	8.3 (1.2)	0.52	0.83
10.7 (OMC-2%)	20 (2.9)	5.6 (1260.1)	15.1 (2.2)	0.46	0.75
	50 (7.3)	9.3 (2086.7)	25.0 (3.6)	0.63	0.5
12.7 (OMC)	10 (1.4)	3.7 (842.9)	10.1 (1.5)	0.55	1.01
	20 (2.9)	4.7 (1058.7)	12.7 (1.8)	0.59	0.63
	50 (7.3)	8.3 (1864.3)	22.3 (3.2)	0.6	0.45
14.7 (OMC+ 2%)	10 (1.4)	3.4 (761.3)	9.1 (1.3)	0.51	0.91
	20 (2.9)	4.5 (1011.8)	12.1 (1.8)	0.56	0.61
	50 (7.3)	7.7 (1741.0)	20.8 (3.0)	0.59	0.42

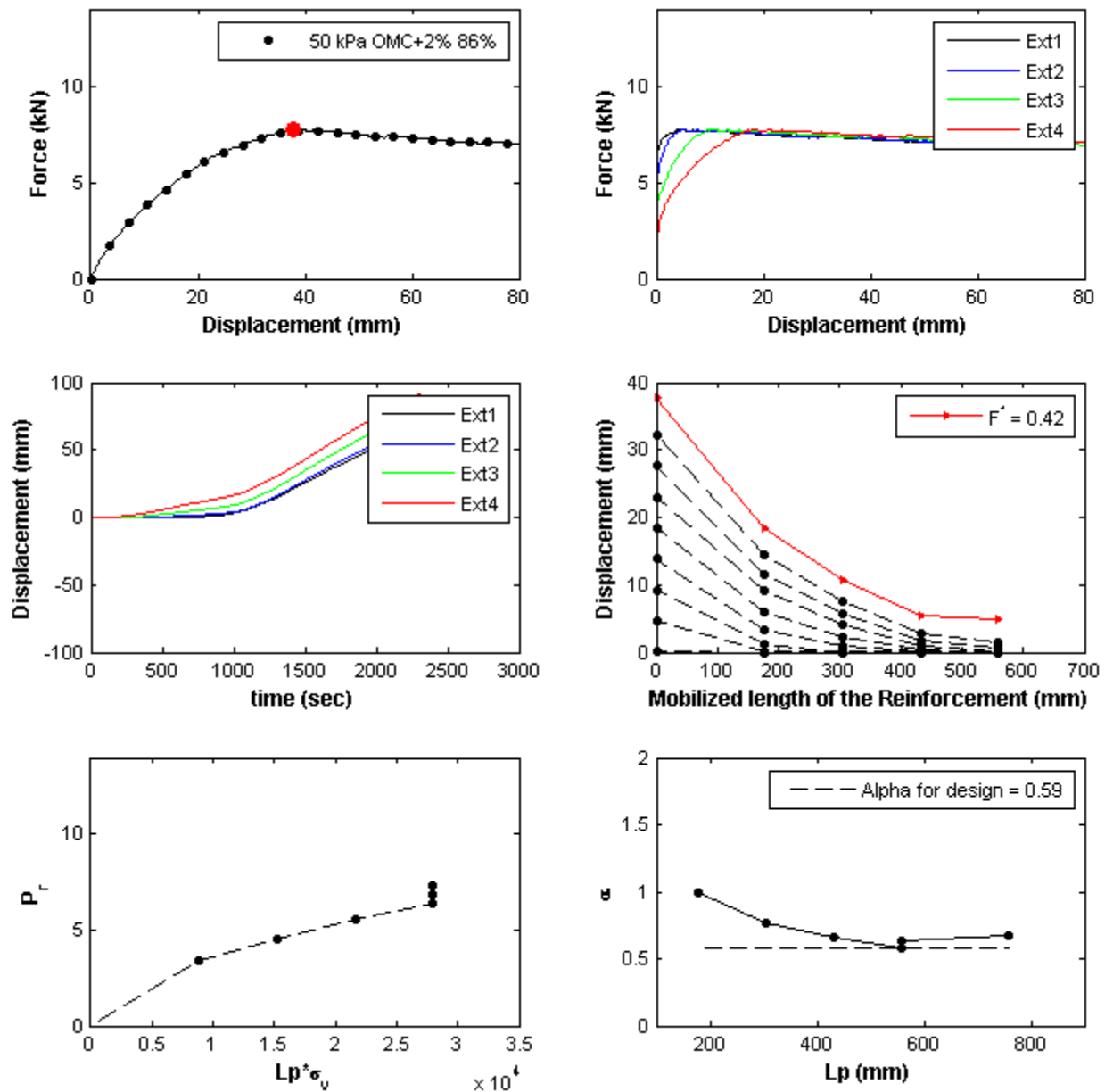


Figure 36. Large-scale pullout test in Minco silt was used to obtain pullout parameters for geotextile HP370 reinforcement and to obtain values for α and F^*

A series of large-scale pullout tests were carried out on a selected marginal soil (Minco silt) and a geotextile fabric (TenCate HP370, woven PP). These tests were carried out at three different moisture content values (OMC-2%, OMC and OMC+2%). The objective of this study was to examine the influence of matric suction on the shear strength and response of soil-geotextile interfaces. The differences in the geotextile

pullout resistance among these cases with different moisture content and suction values were used to propose a moisture reduction factor [MRF - $\mu(\omega)$] in **Equation 1** that accounts for loss of reinforcement pullout resistance due to increased moisture content (see **Figure 45** in the **Section 6**). Based on the results of large scale pullout tests, the following conclusions and observations are made:

Consistently greater maximum reinforcement pullout resistances were obtained at OMC-2% than for OMC and OMC+2% for overburden pressure magnitudes of 10 kPa, 20 kPa and 50 kPa. As expected, increasing suction led to higher maximum reinforcement pullout resistances in identical test specimens.

The soil suction data in pullout tests with OMC, OMC-2% and OMC+2% did not indicate any clear dependence of the soil suction on the overburden pressure. In addition, no clear variation was observed for the soil suction with pullout displacement.

The increase in the soil moisture content can significantly reduce the reinforcement pullout resistance due to the reduction in soil suction. The moisture reduction factor, $\mu(\omega)$ at OMC+2% was found to be approximately 12% from large-scale pullout tests.

5. Small-Scale Tests

In addition to the original scope of this project involving large-scale pullout tests, a series of small-scale interface shear and pullout tests were performed to develop a better understanding of the influence of soil moisture content on marginal soil-geotextile interfaces using a multi-scale laboratory testing approach. The small-scale tests were carried out on the same sand and Minco silt materials used in the large-scale pullout tests. In addition, these tests were carried out at the same soil moisture contents (OMC-2%, OMC and OMC+2%), unit weight and normal stress magnitudes (10 kPa, 20 kPa and 50 kPa) as those in the large-scale pullout tests (**Table 10**).

Table 10. Small-scale test cases and material properties

<i>Test information</i>	<i>Uniformly graded fine sand</i>	<i>Minco silt (Sandy silt CL-ML)</i>
<i>Type of small-scale test</i>	Direct shear (control set)	Direct shear, Pullout
<i>Geosynthetic reinforcement</i>	TenCate HP370, woven PP	TenCate HP370, woven PP
<i>Overburden pressures, kPa (psi)</i>	10(1.5), 20(2.9), 50(7.3)	10(1.5), 20(2.9), 50(7.3)
<i>Moisture Content</i>	NMC	OMC-2%; OMC; OMC+2%

Displacement-controlled direct shear tests (DST) and pullout tests were carried out using a DST testing equipment at the OU Geotechnical Testing Laboratory (**Figure 37**). The soil in both the DST and pullout tests was placed in a 57.6 mm x 57.6 mm (2.35" x 2.35") square test cell supplied with the test equipment. The lower box of the DST machine was moved at a speed of 1 mm/min to apply the shear load on the specimen. In the pullout tests, the same displacement rate was applied to the geotextile specimen to pull it out of a fixed test cell filled with Minco silt.



Figure 37. Direct shear test cell

5.1. Direct Shear Tests

A series of direct shear tests was carried out using the HP370 woven geotextile in an uniformly graded fine sand as a control set. Sand was prepared for direct shear tests by drying it in air to achieve a natural moisture content, which was determined to be $\omega =$

0.6%. The 57.6 mm x 57.6 mm (2.35" x 2.35") test cell was then filled with 39.5 grams of sand in four layers (158 grams in total) with a compacted thickness of 6-mm (0.25 inch) each.

Another series of direct shear tests was carried out on Minco silt at different moisture content values. To prepare the Minco silt for direct shear testing, it was mixed with water to an optimum moisture content OMC = 12.7%. Direct shear testing was carried out in the same manner as for sand, but using 4 layers of 39.5 grams compacted to 6 mm (0.25 inches) in each layer.

5.1.1. Results

Figure 38 shows shear stress-displacement and failure envelop results from direct shear tests in sand for normal stresses of 10, 20 and 50 kPa. The strength properties of the sand are reported in **Table 11**.

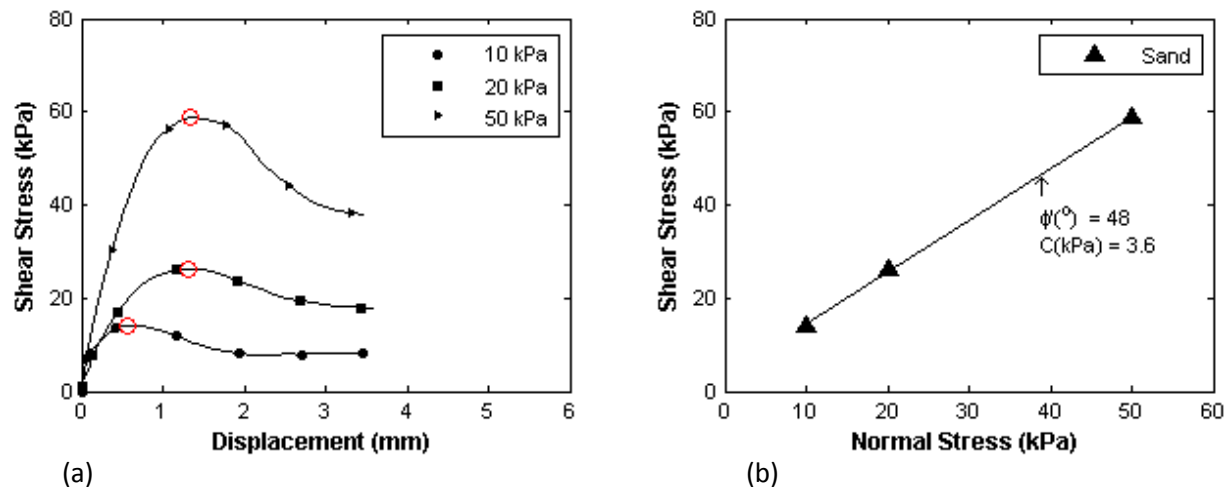


Figure 38. Sand-geotextile interface shear test results: (a) mechanical response; (b) failure envelop

Table 11. Sand strength properties from direct shear tests

$\omega\%$	σ_n kPa (psi)	τ_{max} kPa (psi)	ϕ' ($^\circ$)	C kPa (psi)
	10 (1.4)	14.16 (2.1)		
0.6 (NMC)	20 (2.9)	26.37 (3.8)	47.9	3.6 (0.52)
	50 (7.3)	58.69 (8.5)		

Figure 39 and **Table 12** present the direct shear test results on Minco silt. Results shown in **Figure 39d** indicate that variation of the soil moisture content from OMC-2% to OMC+2% resulted in 2 $^\circ$ reduction in its friction angle. However, the change in the soil cohesion was practically negligible.

The test data on both sand and Minco silt is considered satisfactory. In all test cases, the soil peak strength consistently increases with the overburden pressure. As expected, the friction angle of the sand is greater than that of the Minco silt, and the cohesion of the sand is lower than that of the Minco silt.

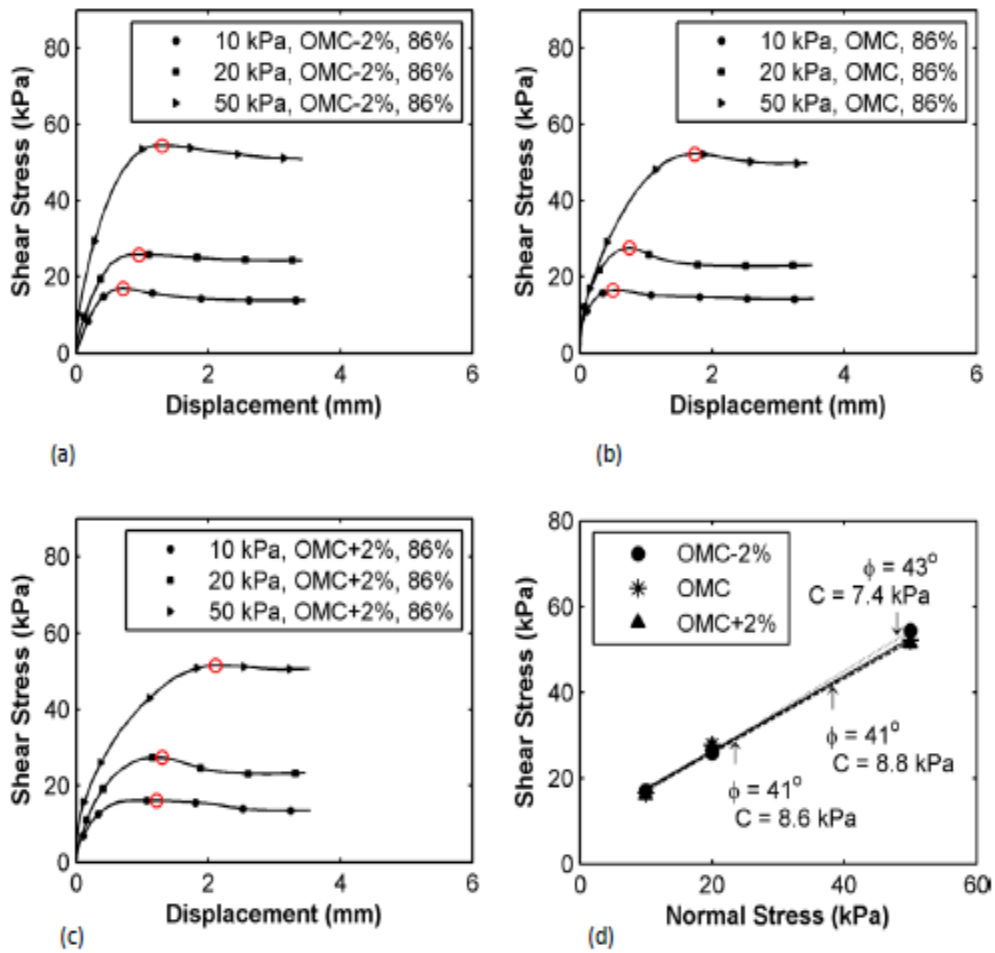


Figure 39. Direct shear test results in Minco silt

Table 12. Minco silt strength properties from direct shear tests

Target ω (%) ⁽¹⁾	σ_n kPa (psi)	ω (%) ⁽²⁾	ψ kPa (psi) ⁽³⁾	\square_{max} kPa (psi)	ϕ' (°) ⁽⁴⁾	C kPa(psi) ⁽⁵⁾
10.7 (OMC-2%)	10 (1.4)	11.0	19 (2.75)	17.02 (2.5)	43.2	7.4 (1.07)
	20 (2.9)	10.7	18 (2.61)	25.89 (3.8)		
	50 (7.3)	10.7	18 (2.61)	54.43 (7.9)		
12.7 (OMC)	10 (1.4)	13.2	12 (1.74)	16.49 (2.4)	41.2	8.8 (1.28)
	20 (2.9)	12.9	12 (1.74)	27.68 (4.0)		
	50 (7.3)	12.8	12 (1.74)	52.22 (7.6)		
14.7 (OMC+ 2%)	10 (1.4)	15.0	10 (1.45)	16.17 (2.4)	40.9	8.6 (1.25)
	20 (2.9)	14.6	10 (1.45)	27.41 (4.0)		
	50 (7.3)	14.4	10 (1.45)	51.52 (7.5)		

Notes: (1) Target moisture content (ω) at OMC \pm 2%, (2) moisture content after direct shear test, (3) suction (ψ) obtained from **Figure 7**, (4,5) from maximum pullout resistance (P_r).

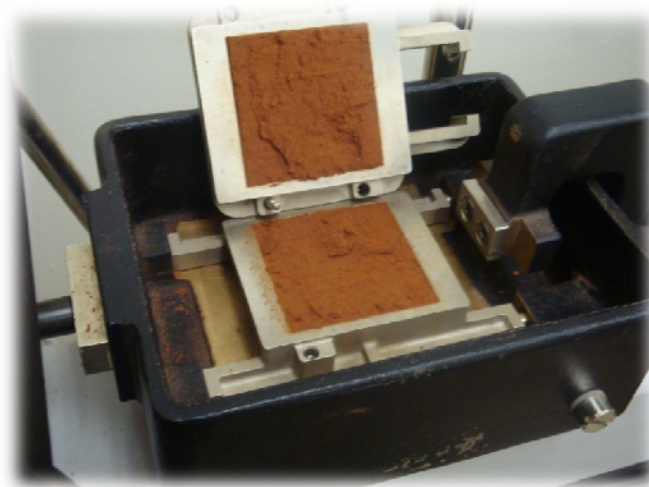


Figure 40. Direct shear in Minco silt

5.2. Pullout Tests

Pullout tests were carried out in Minco silt at OMC-2%, OMC, and OMC+2% (**Figure 41**). The soil at OMC was mixed with a calculated amount of water and its moisture content was measured using the oven method preceding and following each test. The bottom half of the 59.7 mm x 59.7 mm (2.35" x 2.35") test cell was filled with two layers

of Minco silt at the target moisture content and compacted to 6.4 mm (0.25 in). 39.5 grams of soil was used for each layer.



Figure 41. Small-scale pullout tests in Minco silt

The geotextile was attached to a custom-made clamp mounted on the test box and was embedded 50.8 mm (2”) inside the test cell. A metal spacer was used to maintain a gap within the pullout slot to prevent any frictional contacts within the test cell frame during the pullout process. The top half of the box was filled with 2 more layers of Minco silt using 39.5 grams of soil and compacted to 6.4 mm (0.25 in) for each layer.

The subsequent tests at OMC+2% and OMC-2% were carried out in the same manner, but the soils for these tests were prepared differently, because the soil had already been mixed at OMC. The soil was left to air dry to $\omega = 3.8\%$ and was passed through a No. 4 sieve to remove large, hard clumps. Then, the amount of water that needed to be added to soil to obtain the target moisture content (10.7% or 14.7%) was calculated and mixed with the soil in a bowl. The soil prepared at its target moisture content was then stored in airtight plastic containers to prevent loss of water until it was needed for testing.

5.2.1. Results

Figure 42 shows the plots of shearing force versus displacement for pullout tests in Minco silt at OMC, OMC-2% and OMC+2%. It is observed that similar to the direct

shear tests, the shearing force increases with the normal stress. **Table 13** presents the soil-geotextile interface strength properties obtained from the small-scale tests.

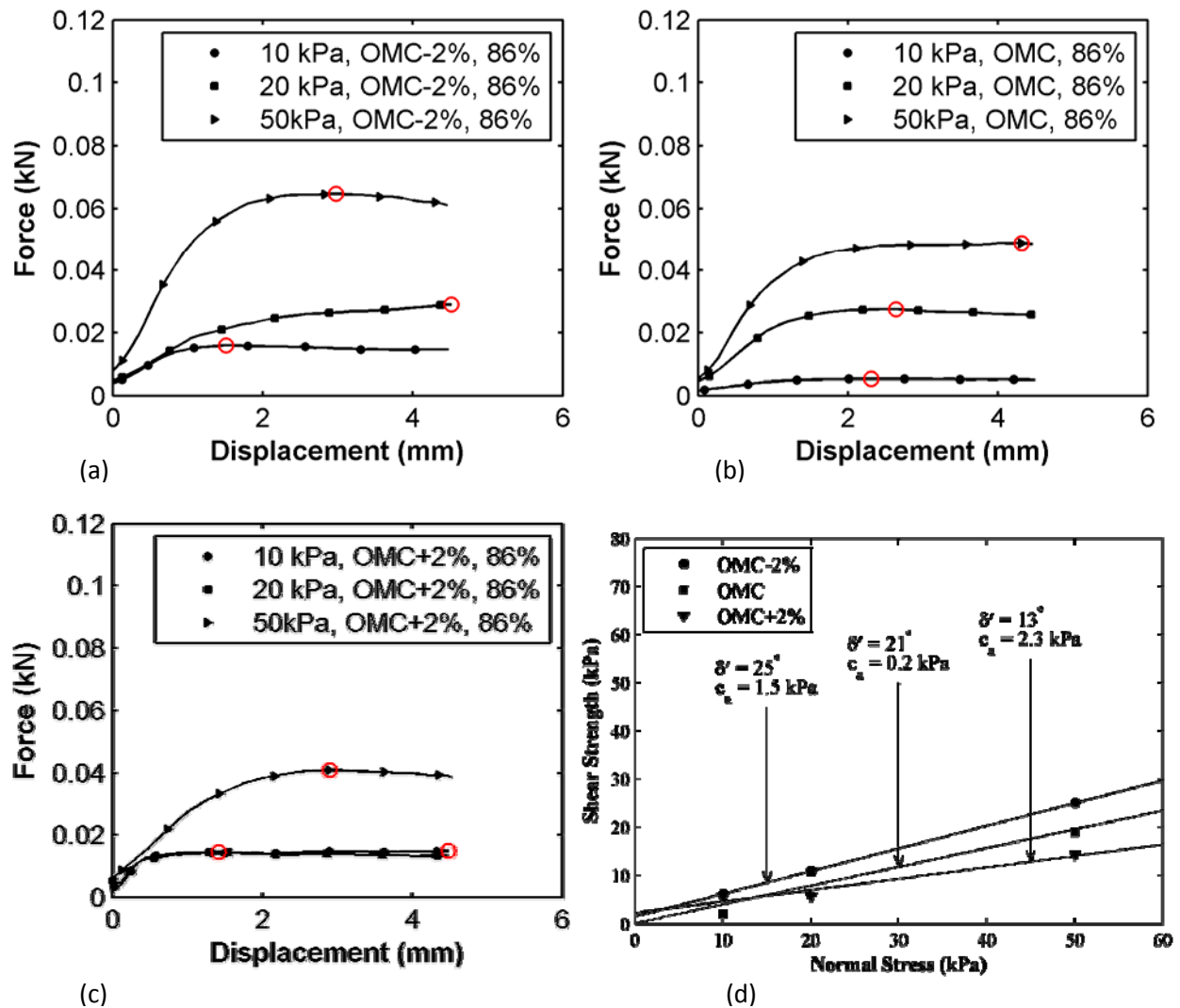


Figure 42. Data for small-scale pullout tests in Minco silt and comparison of failure envelopes of the soil-geotextile interface for determination of effective adhesion (c_a') and friction angle (δ^b) between soil and geotextile interface at different suction values

Table 13. Interface strength properties from small-scale pullout tests

Target ω (%) ⁽¹⁾	σ_n kPa (psi)	ω (%) ⁽²⁾	ψ kPa(psi) ⁽³⁾	τ_{max} kPa (psi)	$\delta^{(4)}$ (°)	C_a (kPa) ⁽⁵⁾
10.7 (OMC-2%)	10 (1.4)	11.0	19 (2.75)	6.2 (0.90)	25	1.5
	20 (2.9)	11.1	19 (2.75)	11.0 (1.60)		
	50 (7.3)	10.6	19 (2.75)	25.1 (3.64)		
12.7 (OMC)	10 (1.4)	12.7	13 (1.89)	2.1 (0.30)	21	0.2
	20 (2.9)	12.9	12 (1.74)	10.7 (1.55)		
	50 (7.3)	13.0	12 (1.74)	19.0 (2.76)		
14.7 (OMC+ 2%)	10 (1.4)	15.0	9 (1.31)	5.6 (0.81)	13	2.3
	20 (2.9)	15.0	9 (1.31)	5.7 (0.83)		
	50 (7.3)	14.8	9 (1.31)	14.4 (2.09)		

Notes: (1) Target moisture content (ω) at OMC \pm 2%, (2) moisture content after pullout test, (3) suction (ψ) obtained from **Figure 7**, (4,5) from maximum pullout resistance (P_r).

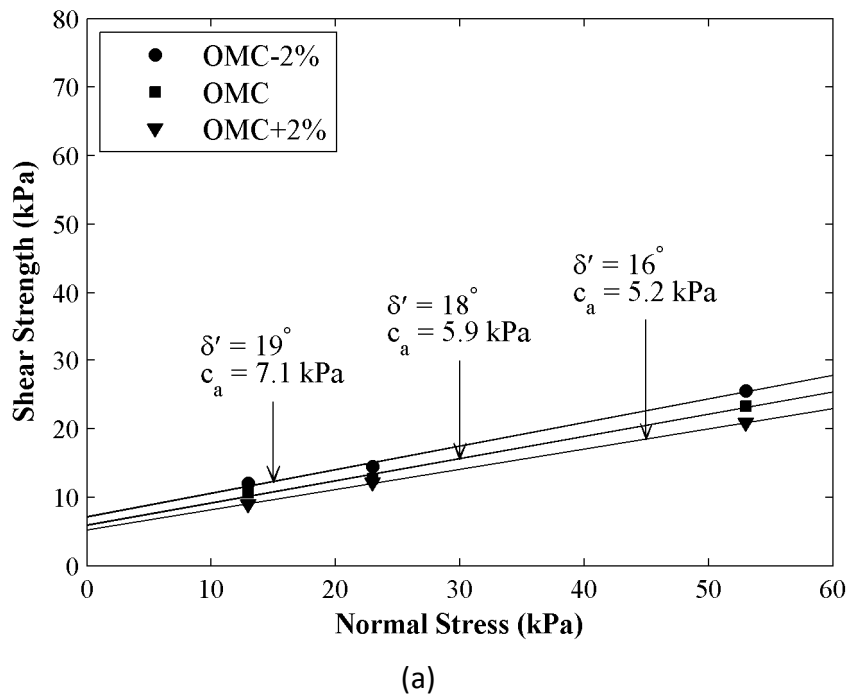


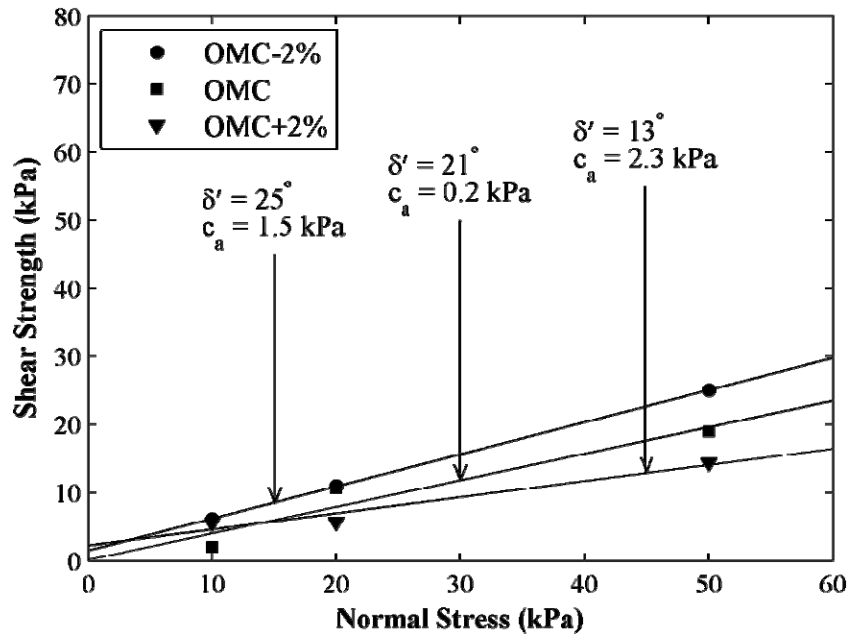
Figure 43. Small-scale pullout test

The interface test results shown in **Table 13** and **Figure 42** show a clear influence of the soil moisture content on the Minco silt-geotextile interface strength properties and pullout resistance. The interface strength properties and pullout resistance decrease as the soil moisture content increases from OMC-2% to OMC+2 %. However, the reduction in interface strength is significant on the wet side of optimum. In other words, there was

a more significant decrease in the interface strength when the moisture content exceeded OMC than the differences between the strength values at OMC and OMC-2%.

Figure 44 shows the graphs of maximum shearing stress versus normal stress for both large-scale and small-scale pullout tests in Minco silt at different moisture content values. Results in **Figures 44** show that the interface friction angle values from both small-scale and large-scale pullout tests are consistently higher for greater soil suction values (i.e. lower soil moisture content). This indicates that the interface friction angle is depends on the soil moisture content. Results shown in **Figure 44** also indicate that the interface friction angle at OMC+2% decreased more significantly in small-scale pullout tests.





(b)

Figure 44. Minco silt-geotextile interface strength results from pullout tests: (a) large-scale tests; (b) small-scale tests

The results in **Figure 44** also indicate a small interface adhesion intercept at large scale and practically negligible interface adhesion at small-scale tests. Larger friction angle and adhesion values are obtained for the interface in the large-scale pullout tests compared to the small-scale. A possible cause for this variation is the size effect on small scale tests. One of the possible reason is the reinforcement length of the geotextile in small-scale is not long enough to achieve the maximum strength before pulling out the geotextile. In pullout test geotextile extensibility results in a no uniform distribution of shear stress and shear displacement along the length of the geotextile this is function of the specimen embedment length (Mallick et al. 1981). The effect of length of embedment is found to be more at lower normal stresses (Mallick et al. 1981; Rao et al. 1988; Alfaro et al. 1995). This characteristic of the geotextile to be extensible produce much lower peak strength in pullout tests compared with the strength from direct shear. Moreover, the value from pullout test decreases with an increase in normal pressure because of the elongation of the reinforcement and a change in the embedment length (Mallick et al. 1981).

6. Moisture Reduction Factor, $\mu(\omega)$

Based on the results of this study, **Equation 1** is modified in the form:

$$P_r = F^* \alpha \sigma'_v L_e C \mu(\omega) \quad (3)$$

Where $\mu(\omega)$ is the $\mu(\omega)$ Moisture Reduction Factor and other terms are as defined previously. **Figure 45** shows the variation of $\mu(\omega)$ with the interface moisture content with the pullout resistance at $\omega = \text{OMC} - 2\%$ taken as the reference value. The results shown in **Figure 45** indicate that wetting of the soil-geotextile interface during construction or service life of the reinforced soil structure can reduce the interface friction angle and pullout resistance significantly. The magnitude of this reduction has been determined to be approximately 33% and 12%, from small-scale and large-scale pullout tests, respectively. Additional tests are in progress to examine the scale effects on $\mu(\omega)$. Nevertheless, both series of tests indicate that $\mu(\omega)$ decreases linearly with ω over the range of moisture content values examined in this study. The test results on Minco silt-geotextile interfaces in this study indicated that the change in moisture content influences the reinforcement pullout resistance. The test results showed that soil compaction at OMC-2% yields greatest interface strength resulting in greatest reinforcement pullout resistance from all the tests.

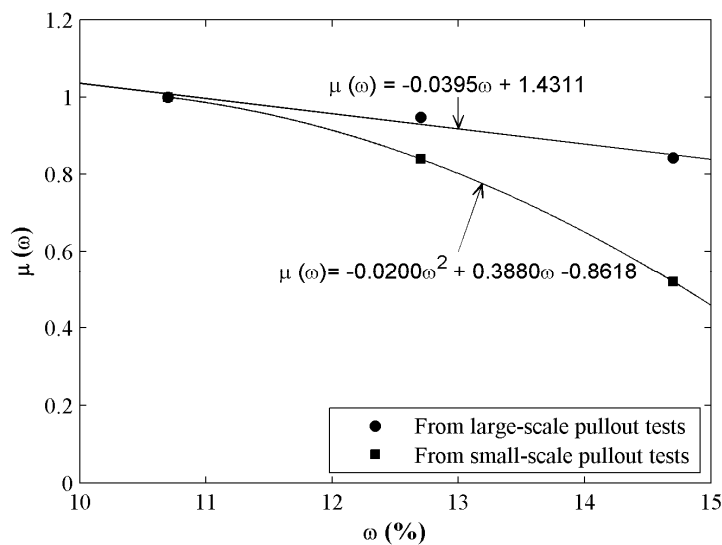


Figure 45 Moisture reduction factor, $\mu(\omega)$, for Minco silt-woven geotextile from large-scale and small-scale pullout tests

7. Conclusions

The primary objective of this study was to develop a moisture reduction factor [MRF - $\mu(\omega)$] for the pullout resistance of soil-geotextile interfaces for the design of reinforced soil structures with marginal soils. Both large-scale and small-scale test results on Minco silt-geotextile interfaces in this study indicated that the change in moisture content influences the reinforcement pullout resistance. The test results showed that soil compaction at OMC-2% yields greatest interface strength resulting in greatest reinforcement pullout resistance. The results also indicate that wetting of the soil-geotextile interface during construction or service life of the reinforced soil structure can reduce the interface friction angle and pullout resistance considerably.

8. Recommendations and Technology Transfer

Based on the results of this study, a moisture reduction factor was proposed for the current FHWA design equation for pullout resistance to account for the reduction in soil-reinforcement interface strength as a result of wetting. The values of the moisture reduction factor, $\mu(\omega)$ were determined through a series of large-scale and small-scale pullout tests. Further testing is in progress to increase the confidence in the proposed MRF equations (i.e. from large-scale and small-scale pullout tests) using a different marginal soil that can be used in reconstruction and/or stabilization of slopes using reinforced soil in Oklahoma. Additional study is also needed to expand the MRF values to include different geosynthetic reinforcement and a wider range of moisture contents for field applications.

This study is in an important first step and part of a long-term study that is aimed at developing a better understanding of the mechanics of unsaturated soil-reinforcement interfaces involving marginal soils. The outcome of this long-term study will help develop reliable procedures to account for wetting-induced loss of soil-reinforcement interface strength to achieve a safer design in the current state of practice. It will assist ODOT and other departments of transportation in the U.S. to include the influence of soil moisture content in their stability analysis and design of reinforced soil structures to

repair, stabilize and reconstruct slopes composed of marginal soils along the transportation corridors in Oklahoma and across the U.S.

9. References

- AASHTO, 2002. Standard specifications for highway bridges. *17th edition. American Association of State Highway and Transportation Officials, Washington, DC, USA, 138-170.*
- Abu-Farsakh, M., Farrag, K., Almohd, I. and Mohiuddin, A., 2005. Bearing and frictional contributions to the pullout capacity of geogrid reinforcements in cohesive backfill. *Proceedings of Geo-Frontiers 2005, ASCE, Austin, TX, 22. <http://cedb.asce.org/cgi/WWWdisplay.cgi?145004>.*
- Alfaro, M.C., Hayashi, S., Miura, N., and Watanabe, K., 1995. Pullout interaction mechanism of geogrid strip reinforcement, *Geosynthetics International, 2(4): 679-698.*
- ASTM International, 2009. Annual Book of Standards, Section 4: Construction, Volume 04.13: Geosynthetics. *American Society for Testing Materials, West Conshohocken, PA, USA.*
- Bergado, D.T., Chai, J.C., Abriera, H.O., Alfaro M.C., and Balasubramaniam, A.S. 1993. Interaction between cohesive frictional soil and various grid reinforcements. *Geotextiles and Geomembranes, 12: 327-349.*
- Elias, V., Christopher, B.R. and Berg, R.R., 2001. Mechanically stabilized earth walls and reinforced soil slopes-design and construction guidelines. *FHWA-NHI-00-043, Federal Highway Administration, Washington, DC, USA. <http://isddc.dot.gov/OLPFiles/FHWA/010567.pdf>*
- Fredlund, D.G., Morgenstern, N.R., and Widger, R.A. (1978), The Shear Strength of Unsaturated Soils, *Canadian Geotechnical Journal, 15(3), 313-321.*
- Keller, G.R., 1995. Experiences with mechanically stabilized structures and native soil backfill. *Transportation Research Record, 1474: 30-38.*
- Koerner, R.M., 2005. *Designing with Geosynthetics, 5th ed. Pearson, Prentice-Hall, New Jersey, USA, 69-294.*
- Mallick, S.B., Zhai, S., Adanur, and Elton, D.J. 1981. Pullout and direct shear testing of geosynthetic reinforcement: State of the Art Report. *Transportation Research Record 1534: 80-90.*
- Miller, G.A. and Hamid, T.B., 2005. Direct shear testing of interfaces in unsaturated soil. *Proceedings of EXPERUS 2005, International Symposium on Advances in Experimental Unsaturated Soil Mechanics, Trento, Italy, June 27-29, 2005, Taylor and Francis Group, plc., London, UK: 111-116.*
- Ou, F-L., Cox, W. and Collett, L. 1982. Rock aggregate management planning for energy conversation: Optimization methodology, *Transportation Research Record, 872: 63-69.*
- Palmeira, E. M., 2004. Bearing force mobilization in pullout tests in geogrids, geotextiles and geomembranes, *22: 481-509.*

Rao, V. and Pandey S.K. 1988. Evaluation of geotextile-soil friction. *Indian Geotechnical Journal.*, 18(1): 77-105.

Tan, N. 2005. Pressuremeter and cone penetrometer testing in a calibration chamber with unsaturated Minco silt, *PhD Dissertation, CEES, OU, OK, USA.*
<http://gradworks.umi.com/31/63/3163317.html>